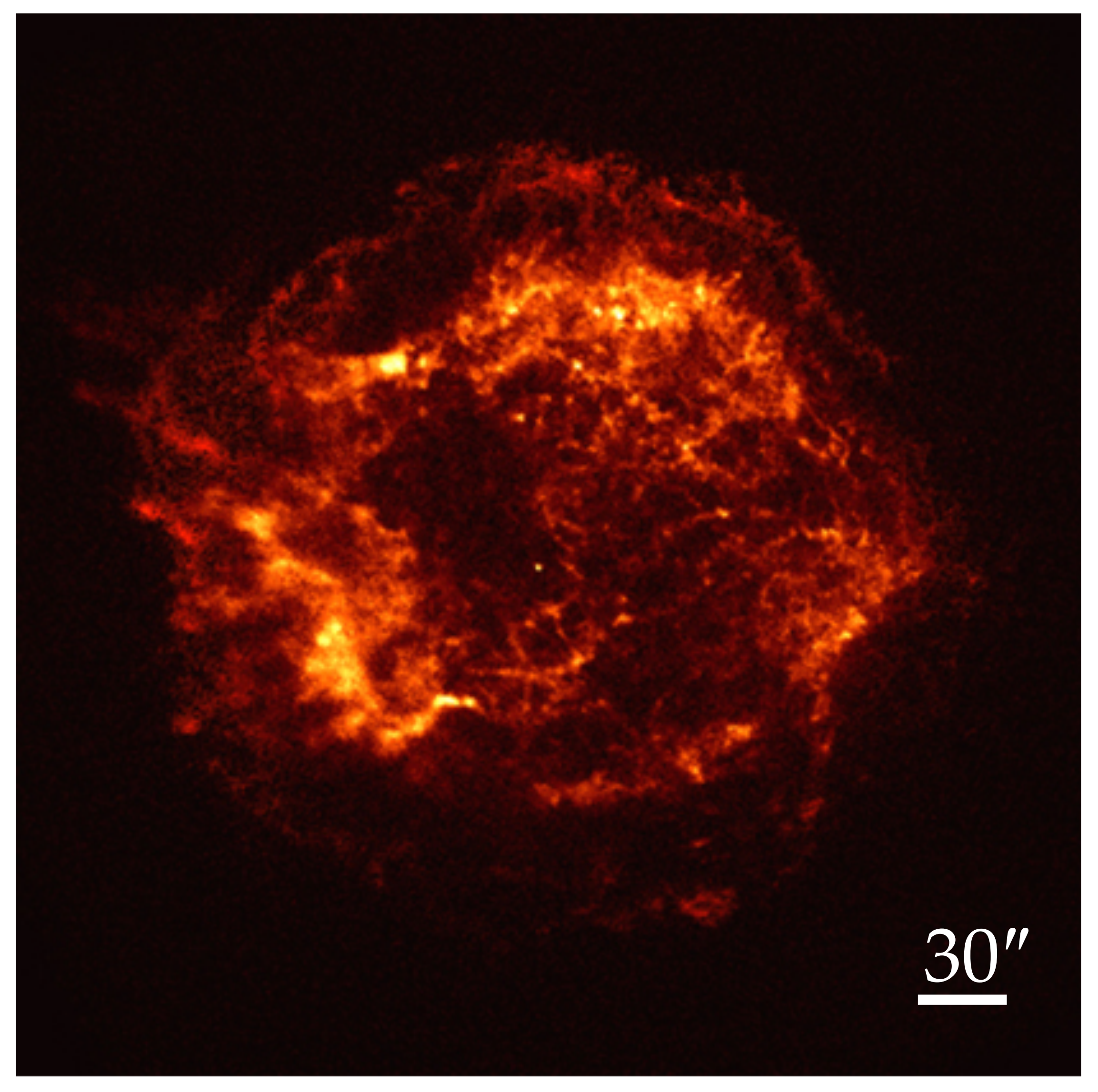

The Supernova Remnant Cas A
3.4 kpc (Milky Way)

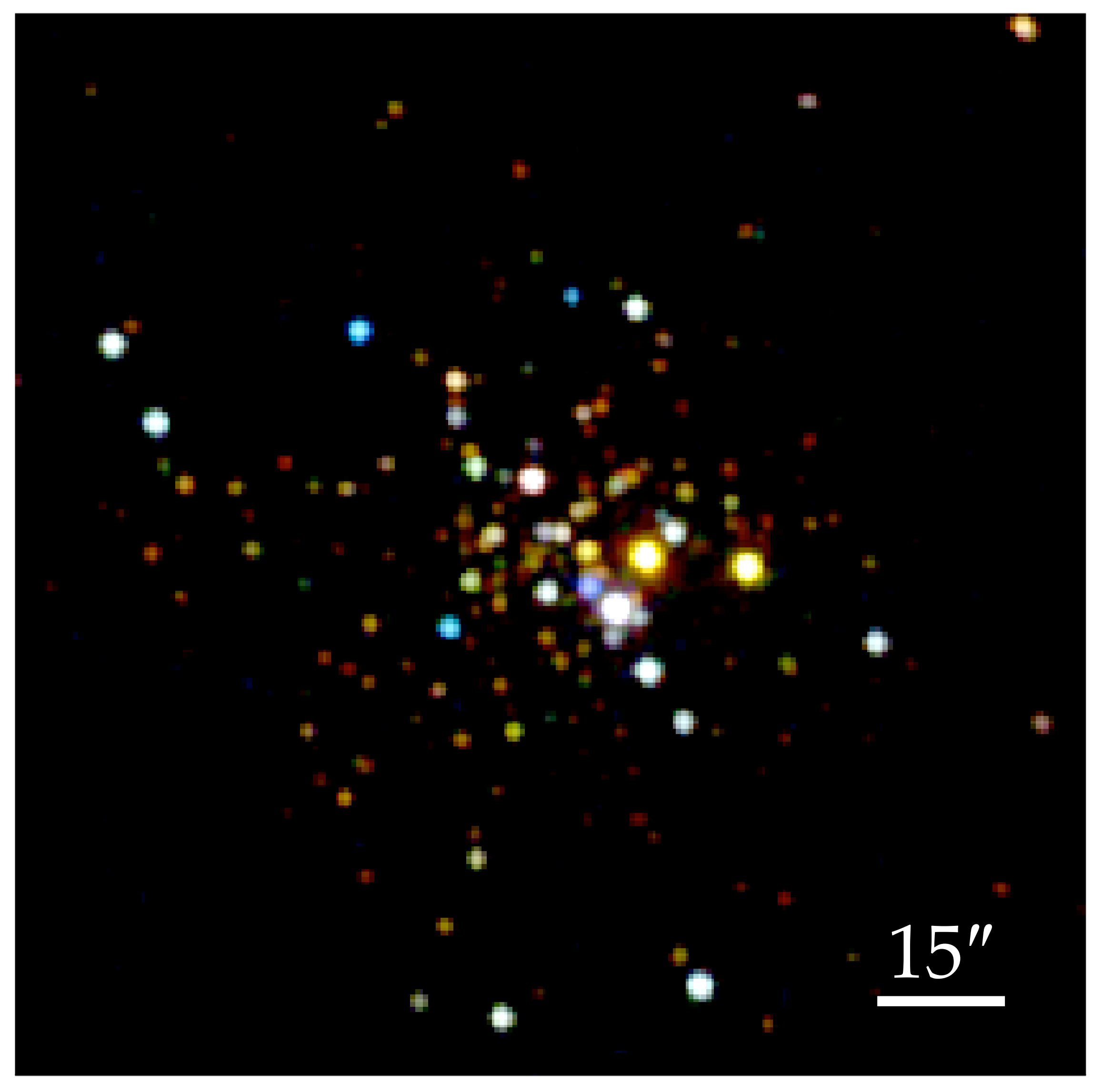

The Globular Cluster 47 Tuc
4.45 kpc (Milky Way)

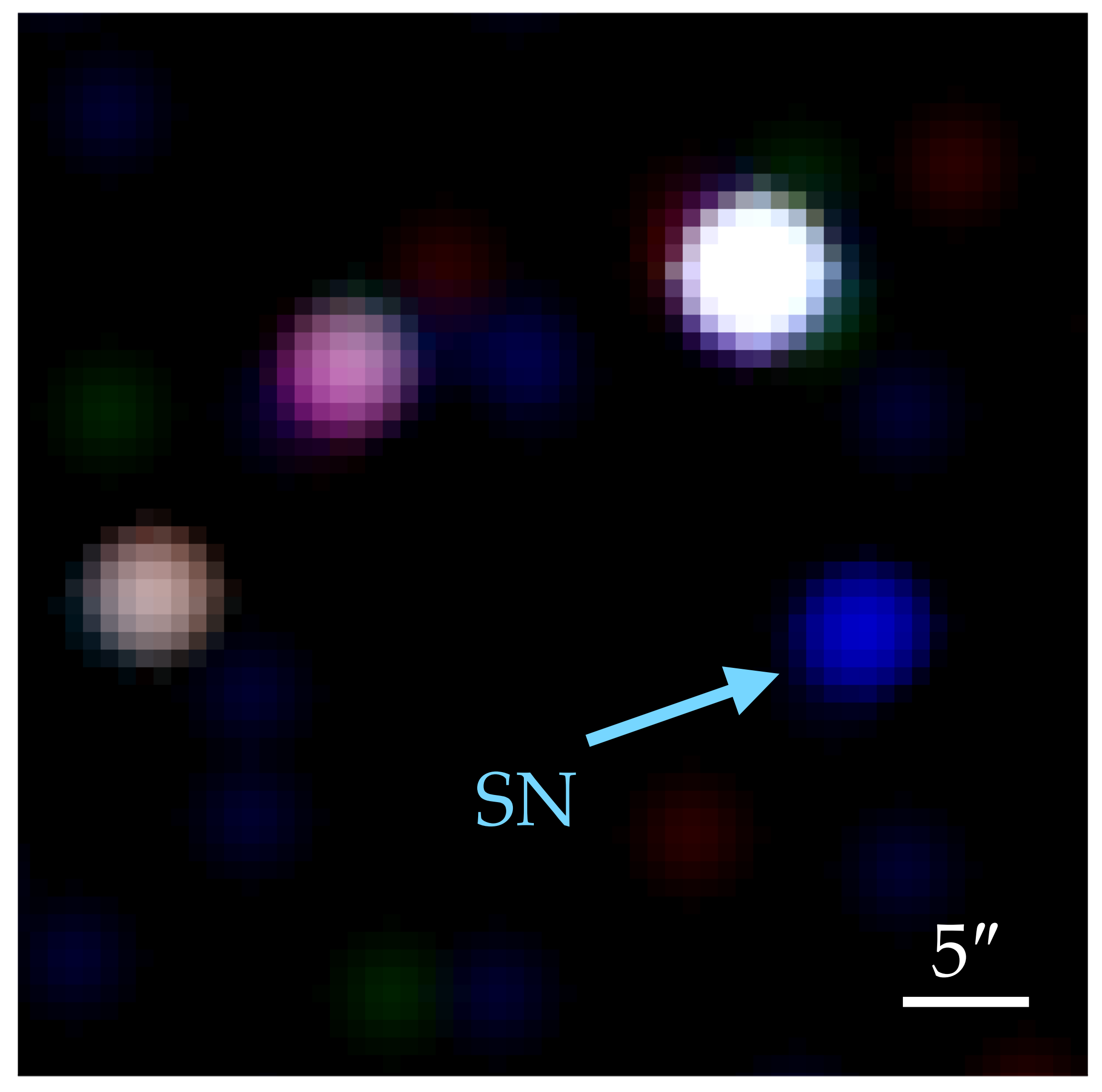

The Type Ib SN 2006jc
26 Mpc (UGC 4904)

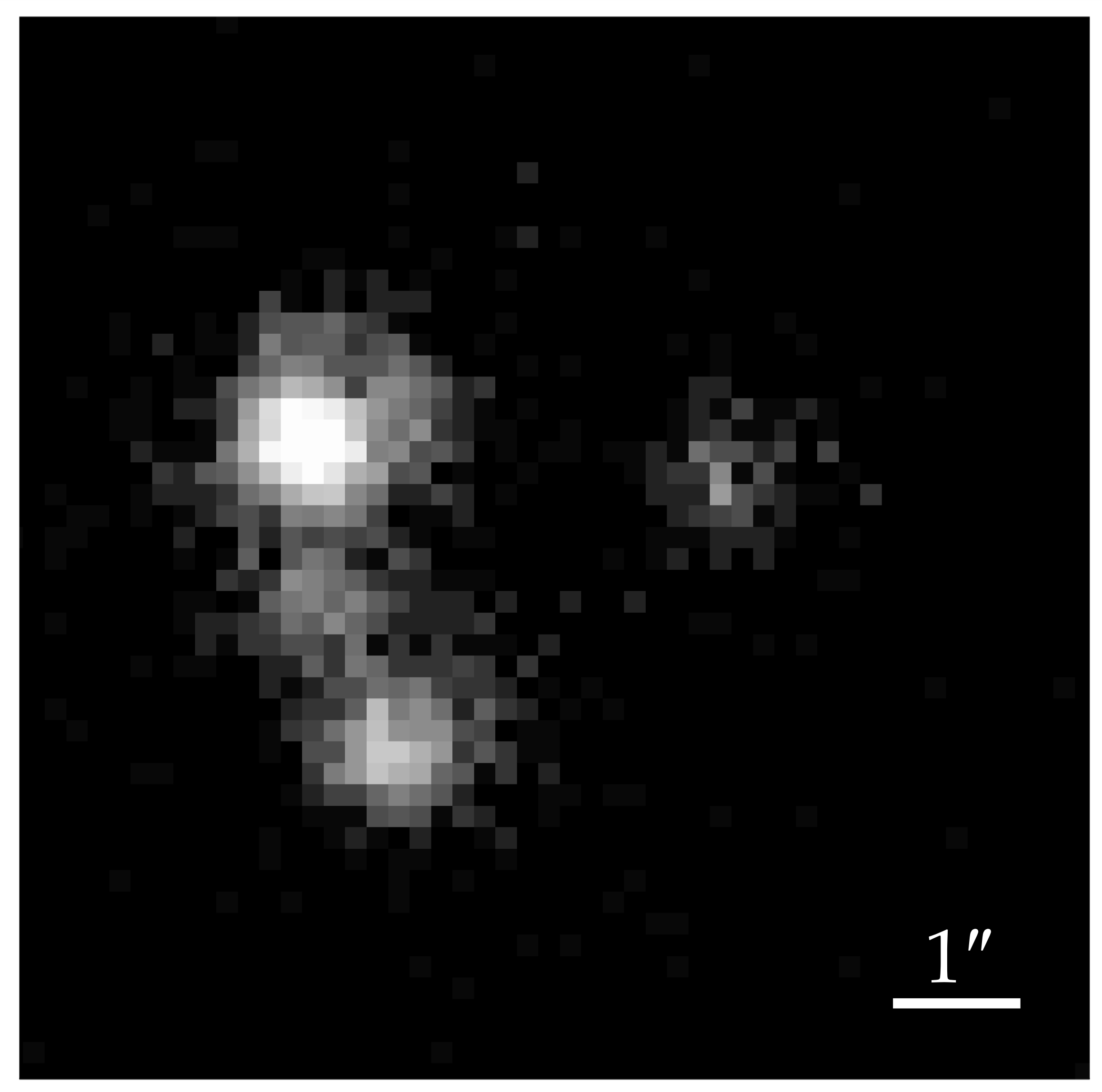

The Lensed Quasar RX J1131−1231
1.4 Gpc ($z = 0.658$)

Unique Discoveries Enabled by *Chandra*'s Angular Resolution

David Pooley
Trinity University &
Eureka Scientific, Inc.

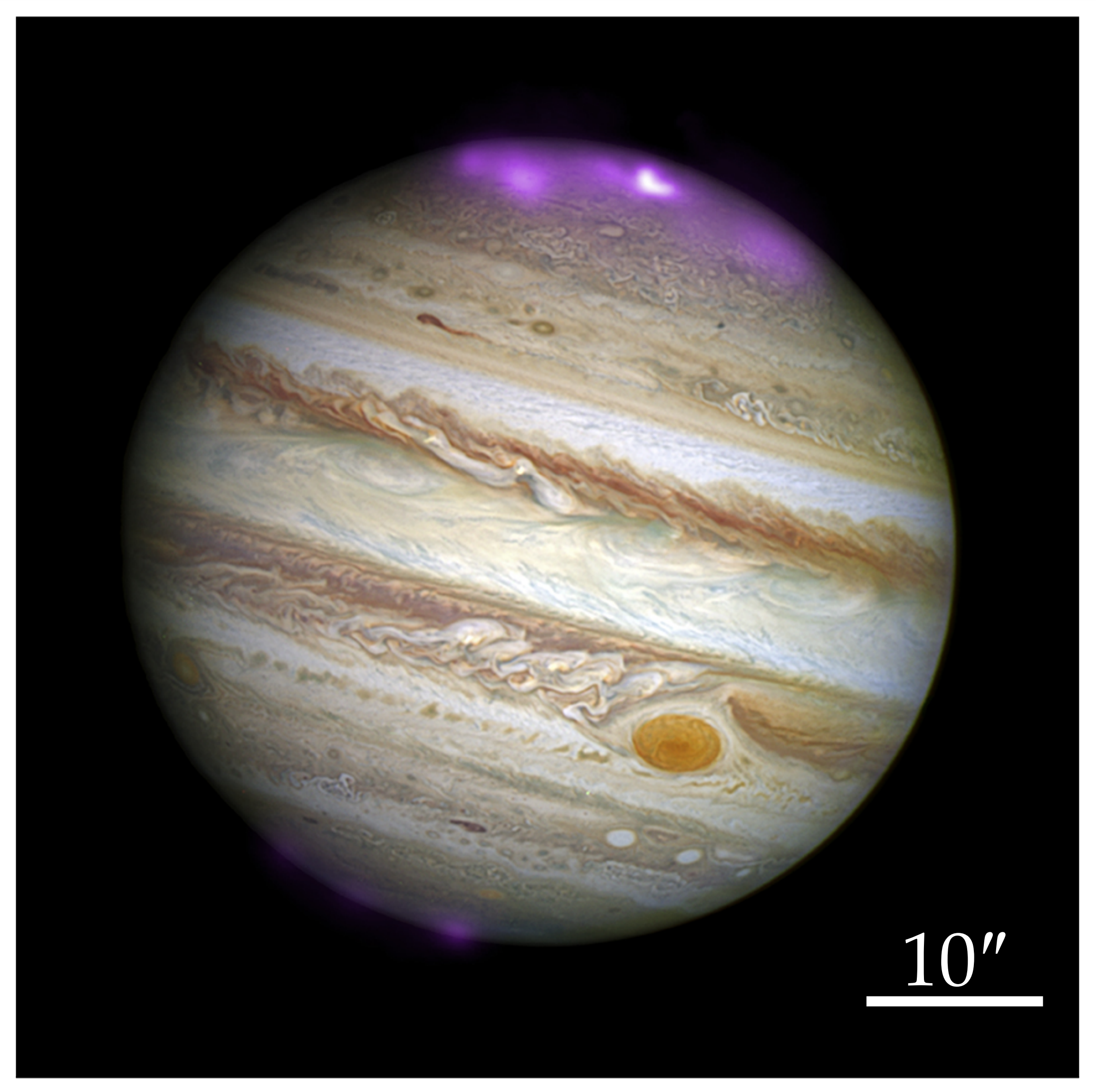

The Planet Jupiter
$6{\times}10^8$ km (Solar System)

The Chandra Deep Field South
up to 8.3 Gpc (up to $z = 5.78$)

Chandra Pinpoints Auroras on Jupiter

- Previous X-rays from Jupiter were thought to be caused by ions coming from close to Io's orbit, but *Chandra* showed auroral X-rays concentrated at poles, suggesting ions come from much further away (e.g., Gladstone et al. 2002).
- Spectra suggested the ions were accelerated to high energies above the poles; high intensity of X-rays is incompatible with solar wind (e.g., Elsner et al. 2005).
- Strong solar activity can also trigger auroras on Jupiter (e.g, image at right), and the northern and southern auroral regions were seen to pulsate independently (Dunn et al. 2017).
- Joint observations with Juno showed link between solar wind compression of magnetosphere and production of auroral X-rays (McEntee et al. 2023).

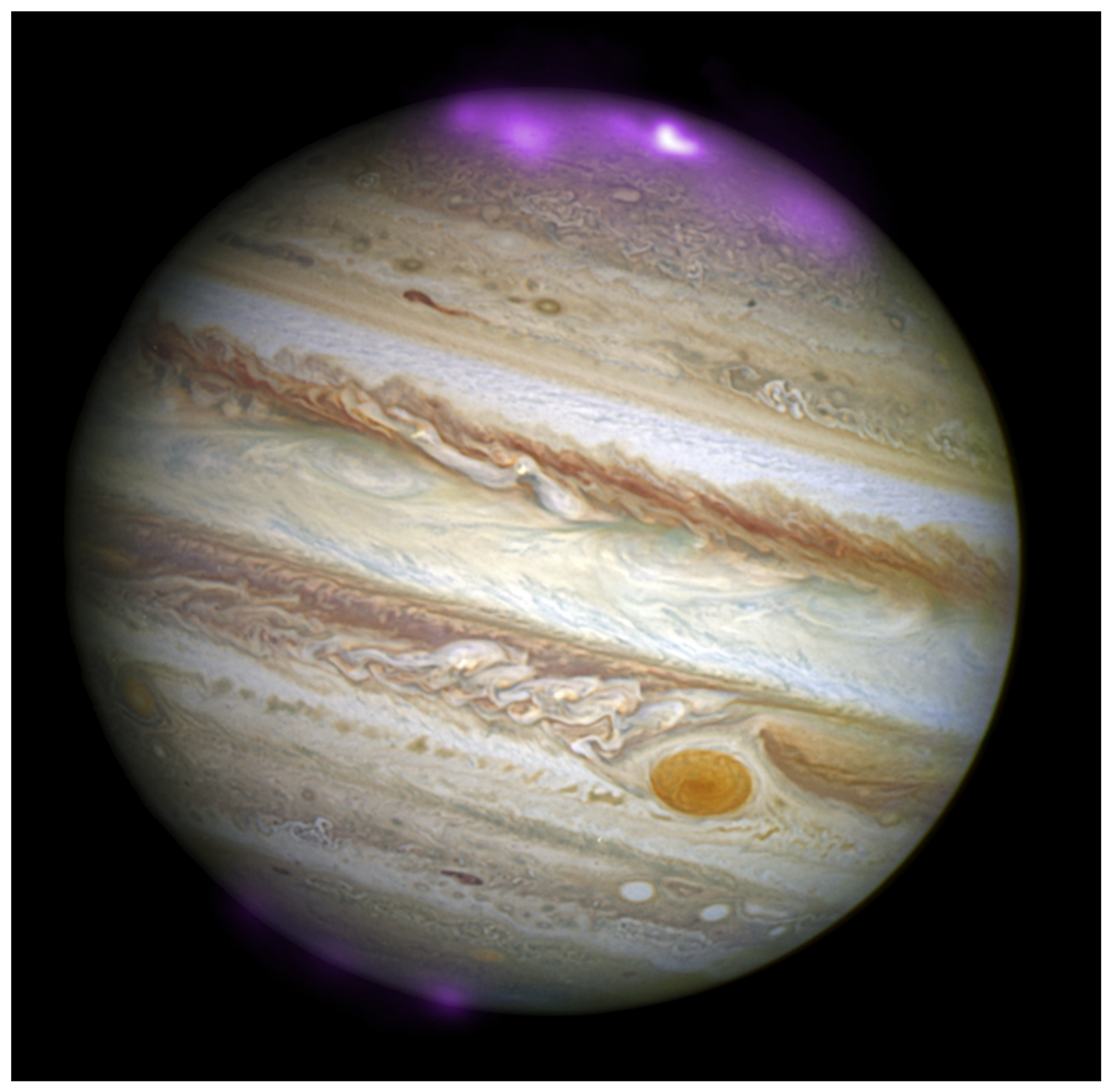

Credit: X-ray: NASA/CXC/UCL/W.Dunn et al, Optical: NASA/STScI

Central Compact Objects in Supernova Remnants

SNR	CCO	μ_{tot} (mas yr^{-1})	d' (kpc)	v_{proj} (km s^{-1})
G15.9+0.2	CXOU J181852.0−150213	<25	10	<1200
Kes 79	CXOU J185238.6+004020	<19	5.0	<450
Cas A	CXOU J232327.9+584842	35^{+16}_{-15}	3.4	570 ± 260
Puppis A	RX J0822−4300	80.4 ± 7.7	2.0	763 ± 73 [(b)]
G266.1−1.2 (Vela Jr.)	CXOU J085201.4−461753	<300	1.0	<1400
PKS 1209−51/52	1E 1207.4−5209	15 ± 7	2.0	<180
G330.2+1.0	CXOU J160103.1−513353	<9.9	5.0	<230
RX J1713.7−3946	1WGA J1713.4−3949	<48	1.0	<230
G350.1−0.3	XMMU J172054.5−372652	15^{+10}_{-9}	4.5	320^{+210}_{-190}
G353.6−0.7	XMMU J173203.3−344518	...[(d)]	3.2	...[(d)]

Adapted from Mayer & Becker (2021)

- Only *Chandra* can measure their proper motions (Mignani et al. 2007, 2019; Halpern & Gotthelf 2010, 2015; Maxted et al. 2018; Mayer et al. 2020; Mayer & Becker 2021).
- These constrain the kick velocities of the neutron stars and the locations of the explosions (powerful tool for explosion asymmetries and inhomogeneity of the circumstellar environments).

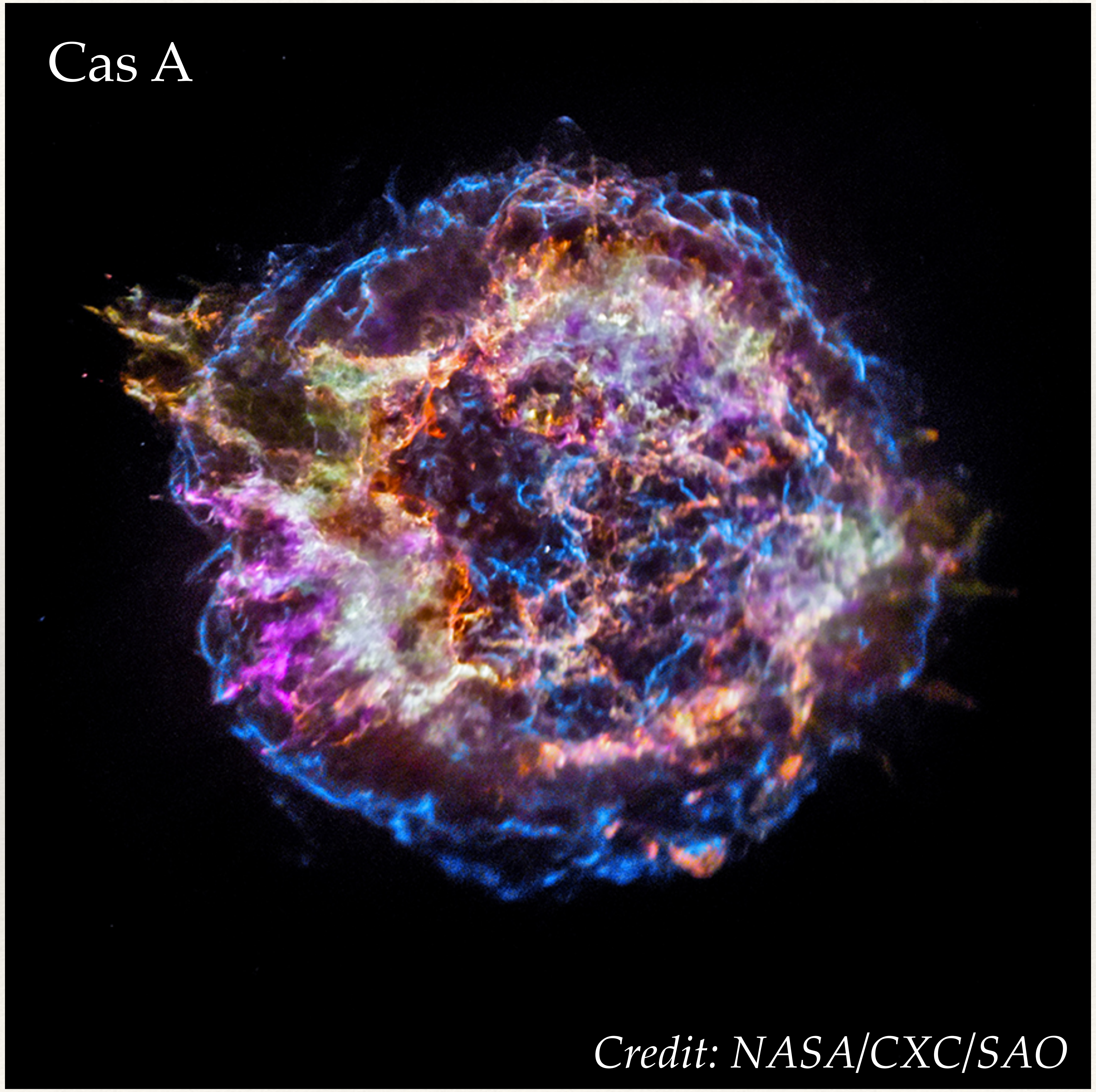

Credit: NASA/CXC/SAO

Chandra Reveals the Ubiquity of Black Holes

- The sensitivity of *Chandra* quickly allowed the cosmic X-ray background to be largely resolved and showed the prevalence of active galactic nuclei throughout the universe in both the Chandra Deep Field South (CDF-S; Giacconi et al. 2001) and the Chandra Deep Field North (CDF-N; Hornschemeier et al. 2001; Brandt et al. 2001).
- With additional observations, the CDF-S has become the deepest X-ray image ever obtained (e.g., Luo et al. 2016; Vito et al. 2016).

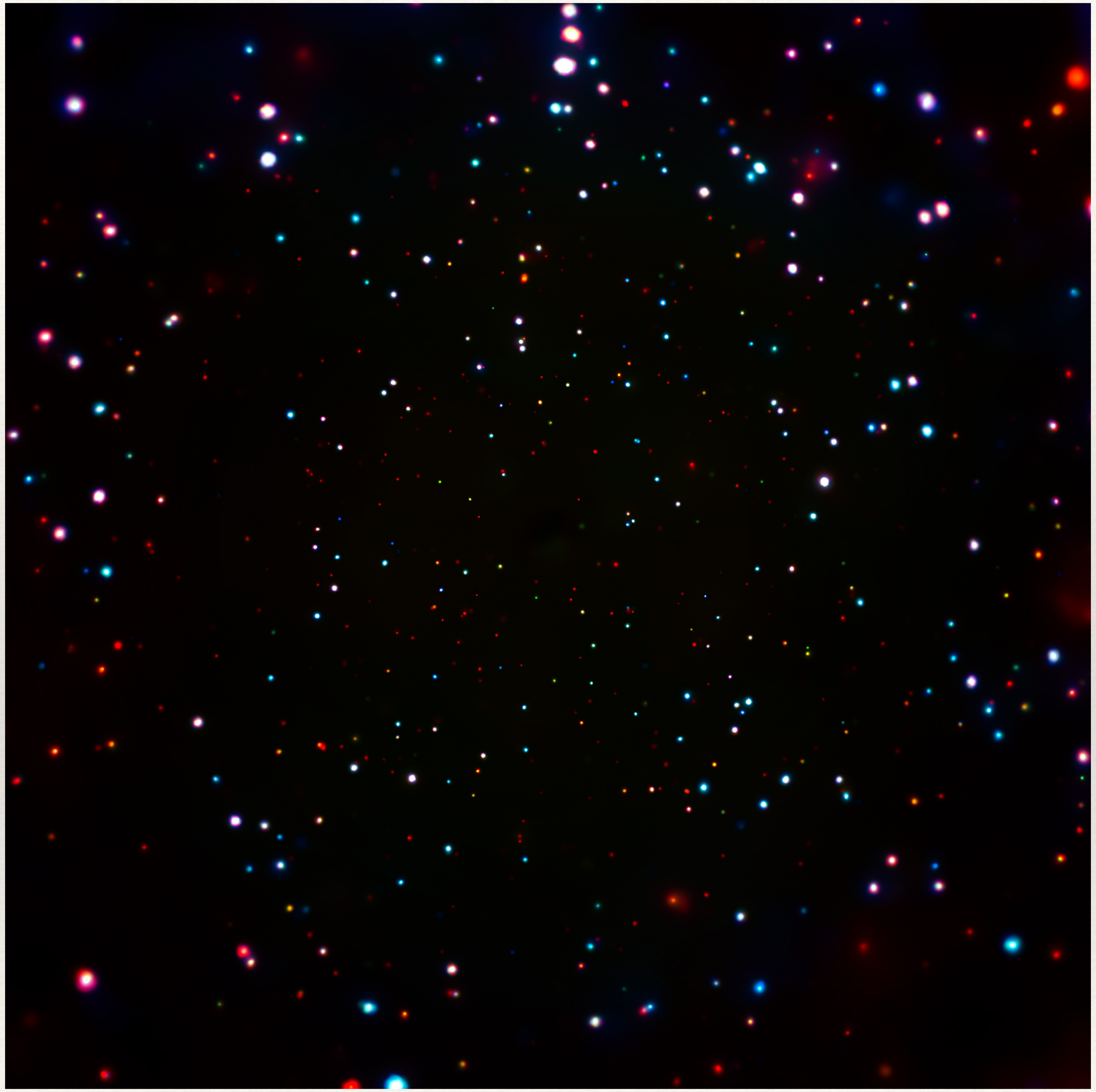

Credit: NASA/CXC/Penn State/B.Luo et al.

Chandra Reveals the Ubiquity of Black Holes

- The sensitivity of *Chandra* quickly allowed the cosmic X-ray background to be largely resolved and showed the prevalence of active galactic nuclei throughout the universe in both the Chandra Deep Field South (CDF-S; Giacconi et al. 2001) and the Chandra Deep Field North (CDF-N; Hornschemeier et al. 2001; Brandt et al. 2001).
- With additional observations, the CDF-S has become the deepest X-ray image ever obtained (e.g., Luo et al. 2016; Vito et al. 2016).
- The CDF-S even has its own wikipedia page with two optical images and no X-ray image!

?????????

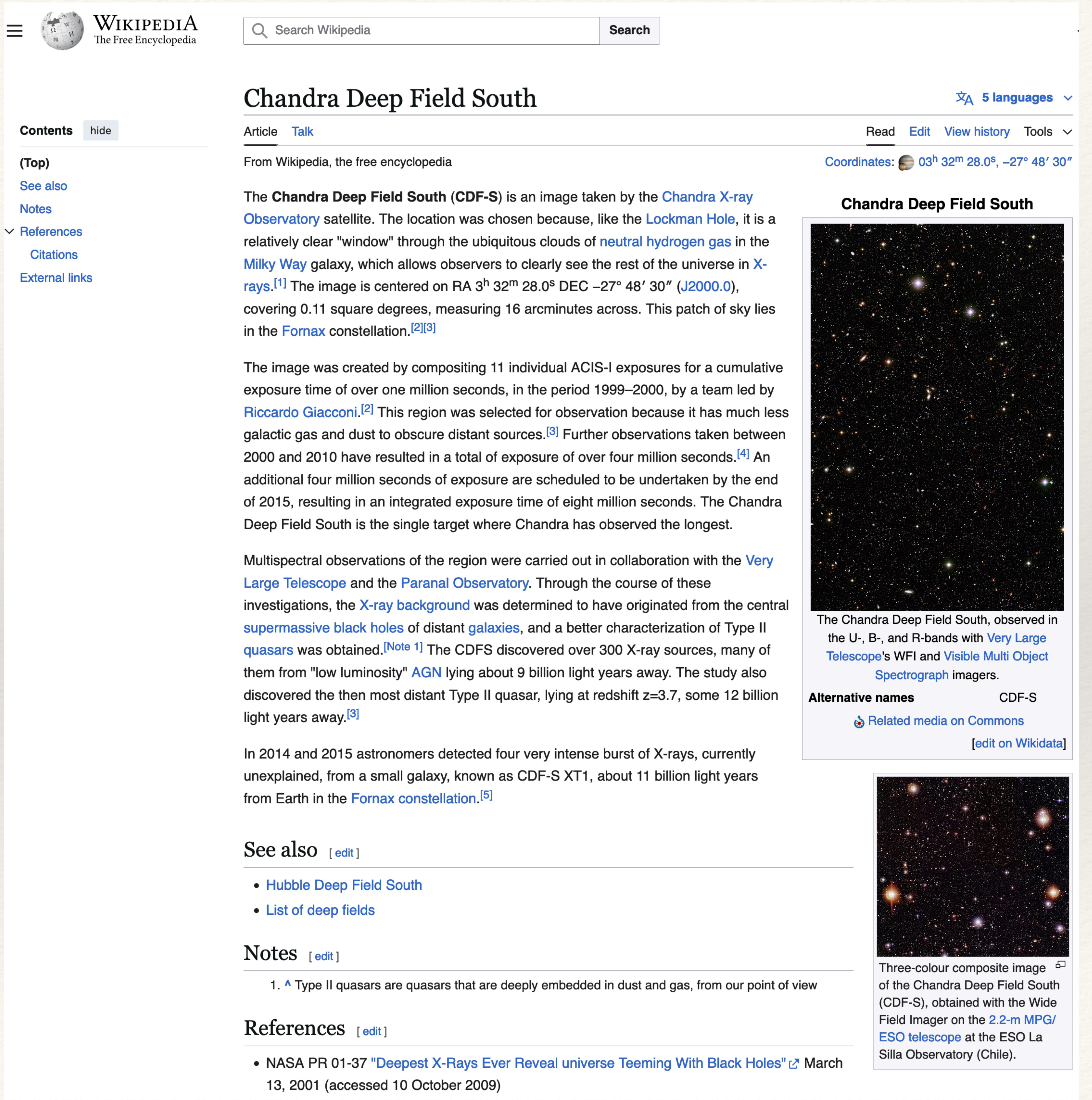
WIKIPEDIA
The Free Encyclopedia

Search Wikipedia | Search

Contents hide

(Top)
See also
Notes
References
Citations
External links

Chandra Deep Field South

5 languages

Article Talk | Read Edit View history Tools

From Wikipedia, the free encyclopedia

Coordinates: 03h 32m 28.0s, −27° 48′ 30″

The **Chandra Deep Field South** (**CDF-S**) is an image taken by the Chandra X-ray Observatory satellite. The location was chosen because, like the Lockman Hole, it is a relatively clear "window" through the ubiquitous clouds of neutral hydrogen gas in the Milky Way galaxy, which allows observers to clearly see the rest of the universe in X-rays.[1] The image is centered on RA 3h 32m 28.0s DEC −27° 48′ 30″ (J2000.0), covering 0.11 square degrees, measuring 16 arcminutes across. This patch of sky lies in the Fornax constellation.[2][3]

The image was created by compositing 11 individual ACIS-I exposures for a cumulative exposure time of over one million seconds, in the period 1999–2000, by a team led by Riccardo Giacconi.[2] This region was selected for observation because it has much less galactic gas and dust to obscure distant sources.[3] Further observations taken between 2000 and 2010 have resulted in a total of exposure of over four million seconds.[4] An additional four million seconds of exposure are scheduled to be undertaken by the end of 2015, resulting in an integrated exposure time of eight million seconds. The Chandra Deep Field South is the single target where Chandra has observed the longest.

Multispectral observations of the region were carried out in collaboration with the Very Large Telescope and the Paranal Observatory. Through the course of these investigations, the X-ray background was determined to have originated from the central supermassive black holes of distant galaxies, and a better characterization of Type II quasars was obtained.[Note 1] The CDFS discovered over 300 X-ray sources, many of them from "low luminosity" AGN lying about 9 billion light years away. The study also discovered the then most distant Type II quasar, lying at redshift z=3.7, some 12 billion light years away.[3]

In 2014 and 2015 astronomers detected four very intense burst of X-rays, currently unexplained, from a small galaxy, known as CDF-S XT1, about 11 billion light years from Earth in the Fornax constellation.[5]

Chandra Deep Field South

The Chandra Deep Field South, observed in the U-, B-, and R-bands with Very Large Telescope's WFI and Visible Multi Object Spectrograph imagers.

Alternative names	CDF-S

Related media on Commons

[edit on Wikidata]

Three-colour composite image of the Chandra Deep Field South (CDF-S), obtained with the Wide Field Imager on the 2.2-m MPG/ESO telescope at the ESO La Silla Observatory (Chile).

See also [edit]

- Hubble Deep Field South
- List of deep fields

Notes [edit]

1. ^ Type II quasars are quasars that are deeply embedded in dust and gas, from our point of view

References [edit]

- NASA PR 01-37 "Deepest X-Rays Ever Reveal universe Teeming With Black Holes" March 13, 2001 (accessed 10 October 2009)

Critical Importance of Close Binaries in Globular Clusters

- 1960s, 70s: Theory predicted the inevitable collapse of cluster of single stars (e.g., Hénon 1961, 1965).
- 1980s: Simulations confirmed this and gave rich understanding of collapse and how **encounters with binaries provide the internal energy to prevent collapse** (e.g., work by Goodman, Heggie, Hut, Spitzer).
- 1970s, 80s: Optical observers found no binaries (e.g., Gunn & Griffin 1979).
- 1990s: Observers found some, but not many, binaries (see Hut et al. 1992 & references therein).

"Heggie's Law"

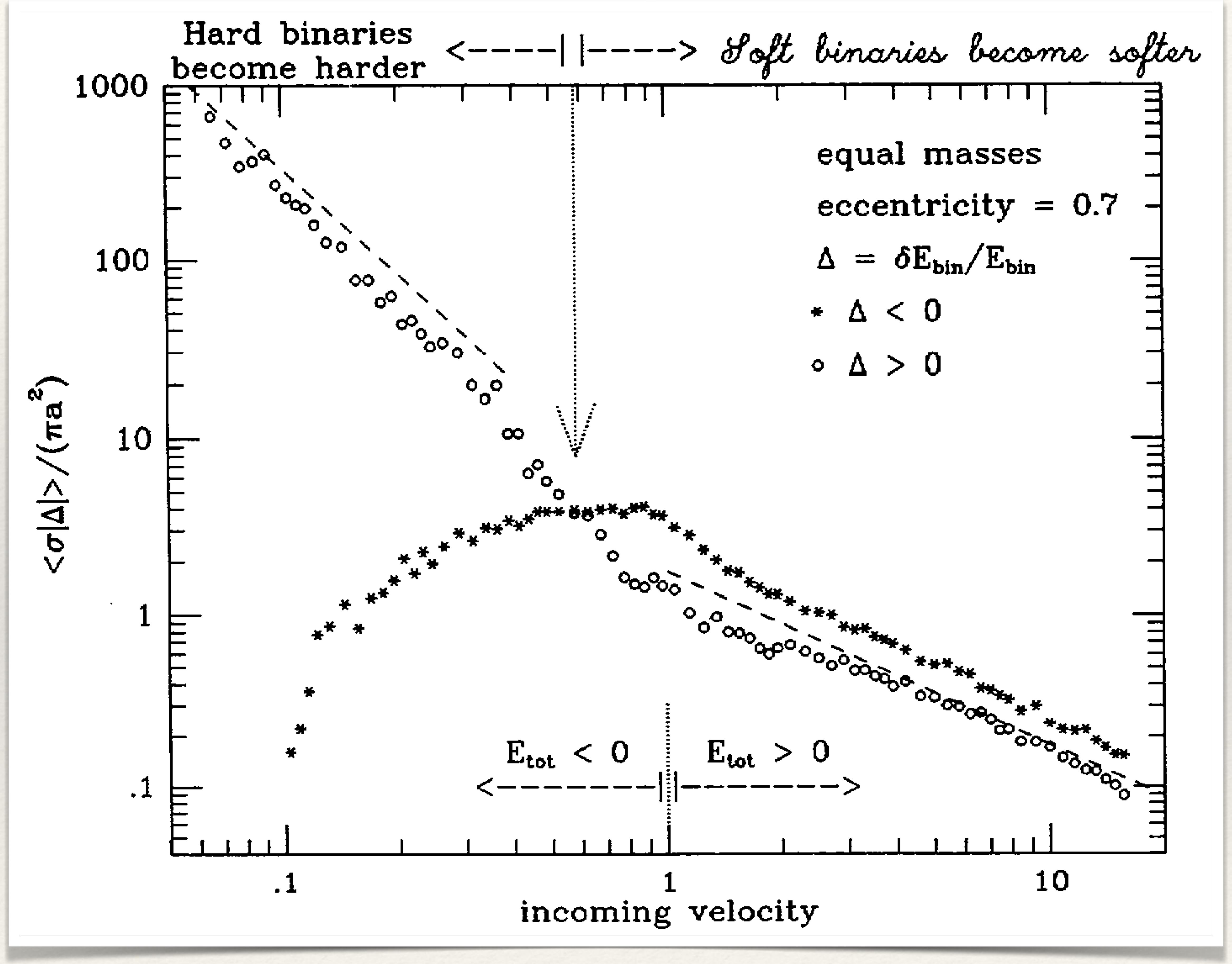

Hut (1983)

Two Big Mysteries in Globular Clusters

- Luminous (>10^{36} erg/s) X-ray sources found in 1970s quickly recognized as overabundant in globular clusters (Gursky 1973; Clark 1975; Katz 1975) due to cluster dynamics (Fabian, Pringle, & Rees 1975; Sutantyo 1975; Hills 1975, 1976; Heggie 1975; Verbunt & Hut 1983).
- Neutron star low-mass X-ray binaries (LMXBs) in outburst.
- Low luminosity (<10^{34} erg/s) X-ray sources discovered in 1980s by *Einstein* (Hertz & Grindlay 1983) and found in greater numbers with *ROSAT* (e.g., Verbunt 2001)
- Suggested to be cataclysmic variables (Hertz & Grindlay 1983), quiescent LMXBs (Hertz & Grindlay 1983, Verbunt et al. 1984), millisecond pulsars (Saito 1997), magnetically active binaries (Bailyn et al. 1997), but only two secure identifications based on *ROSAT* positions.

What are the low-luminosity X-ray sources?

- Theory predicted large numbers of cataclysmic variables (CVs) in globular clusters because they should also be overabundant due to cluster internal dynamics (e.g., Hut & Verbunt 1983; Di Stefano & Rappaport 1994)
- Optical observations failed to uncover more than a handful (e.g., Shara et al. 1996)
- Even when many were discovered with *Chandra*, it was unclear whether they were overabundant (e.g., Townsley & Bildsten 2005; Ivanova et al. 2006).
- Most studies indicate there should be a sizeable (~10^2) population of CVs in every rich cluster (e.g., Di Stefano & Rappaport 1994; Davies 1997; Ivanova et al. 2006; Belloni & Rivera Sandoval 2021), but it remains to be found.

Where are the dynamically formed CVs?

Chandra Observations Solve Them Both

- Verbunt (2001): 57 low-luminosity X-ray sources in *ROSAT* observations of 55 globular clusters.
- Today: Over 1500 low-luminosity X-ray sources in *Chandra* observation of over 80 globular clusters.
- The low-luminosity X-ray sources are a heterogenous mix of quiescent LMXBs, CVs, MSPs, and active binaries.
- The number of X-ray sources in a luminosity-limited sample varies greatly from cluster to cluster.

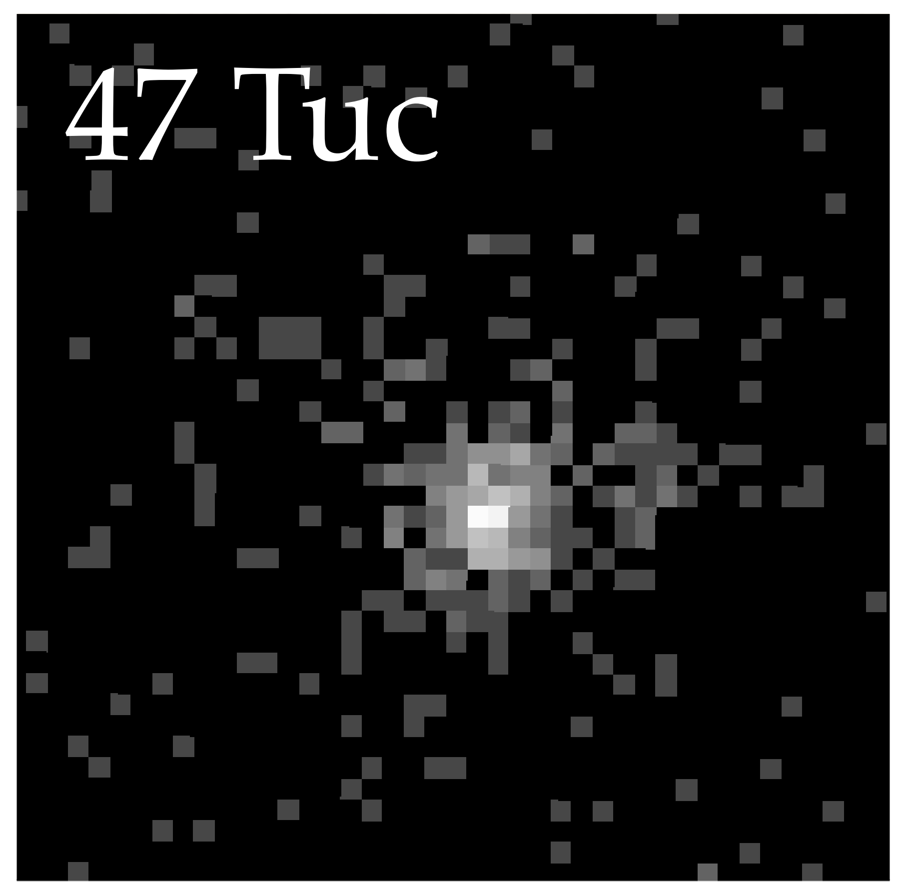

Einstein (8 ksec)

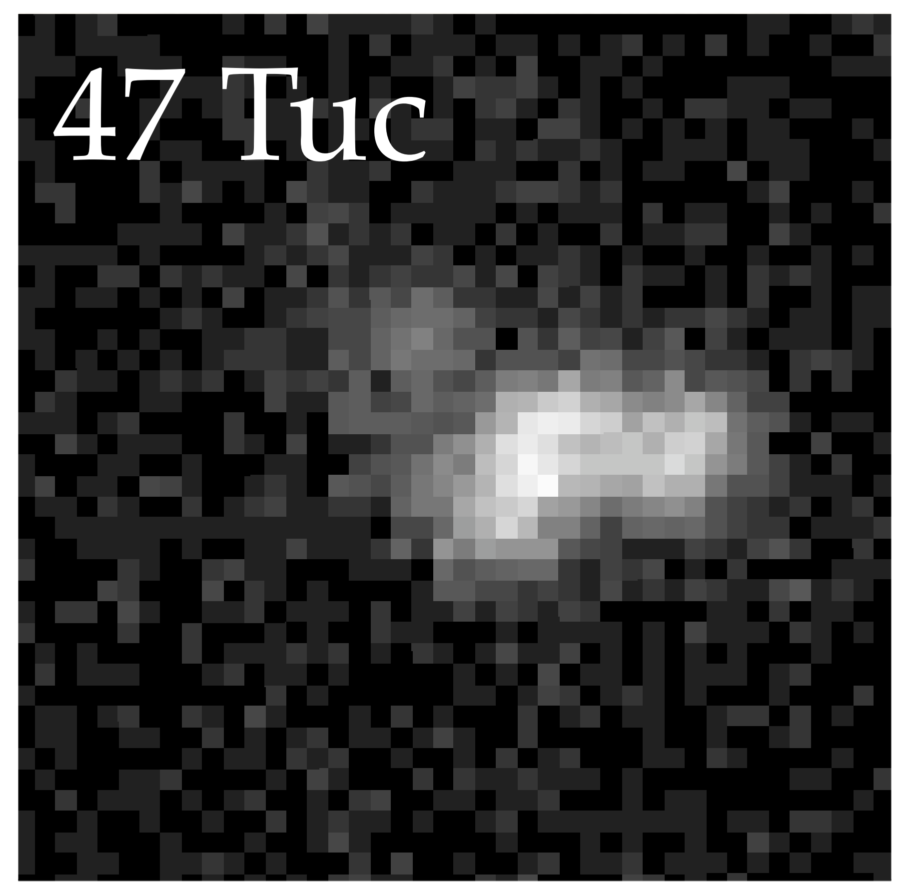

ROSAT (77 ksec)

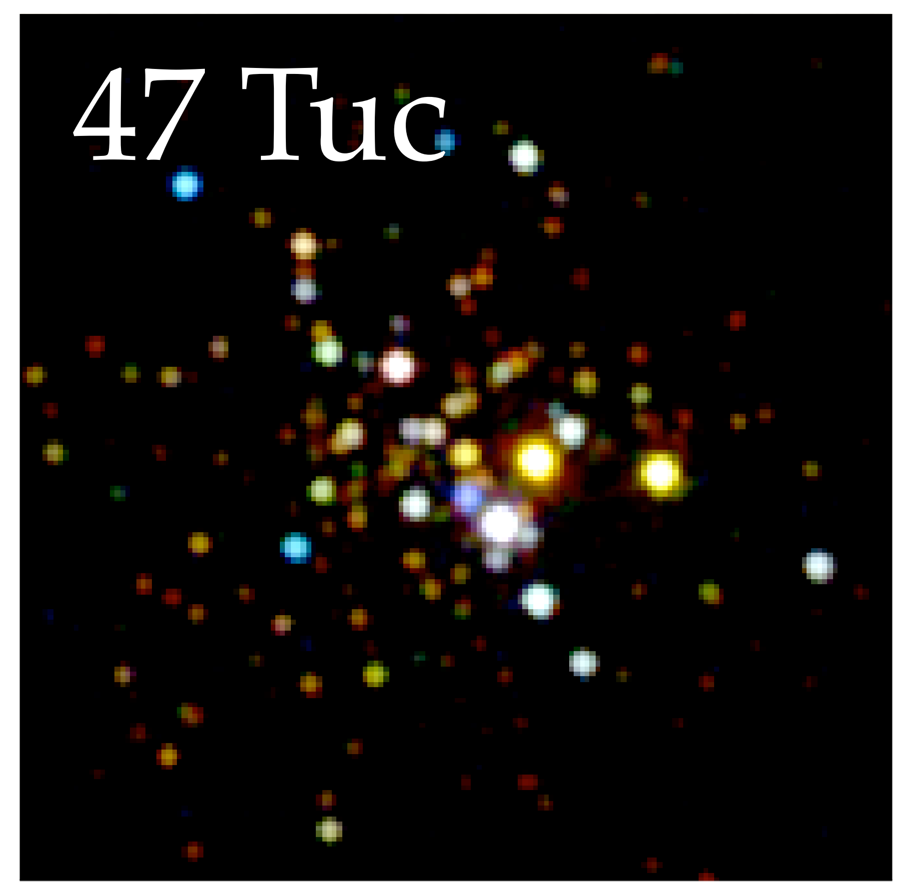

Chandra (240 ksec)

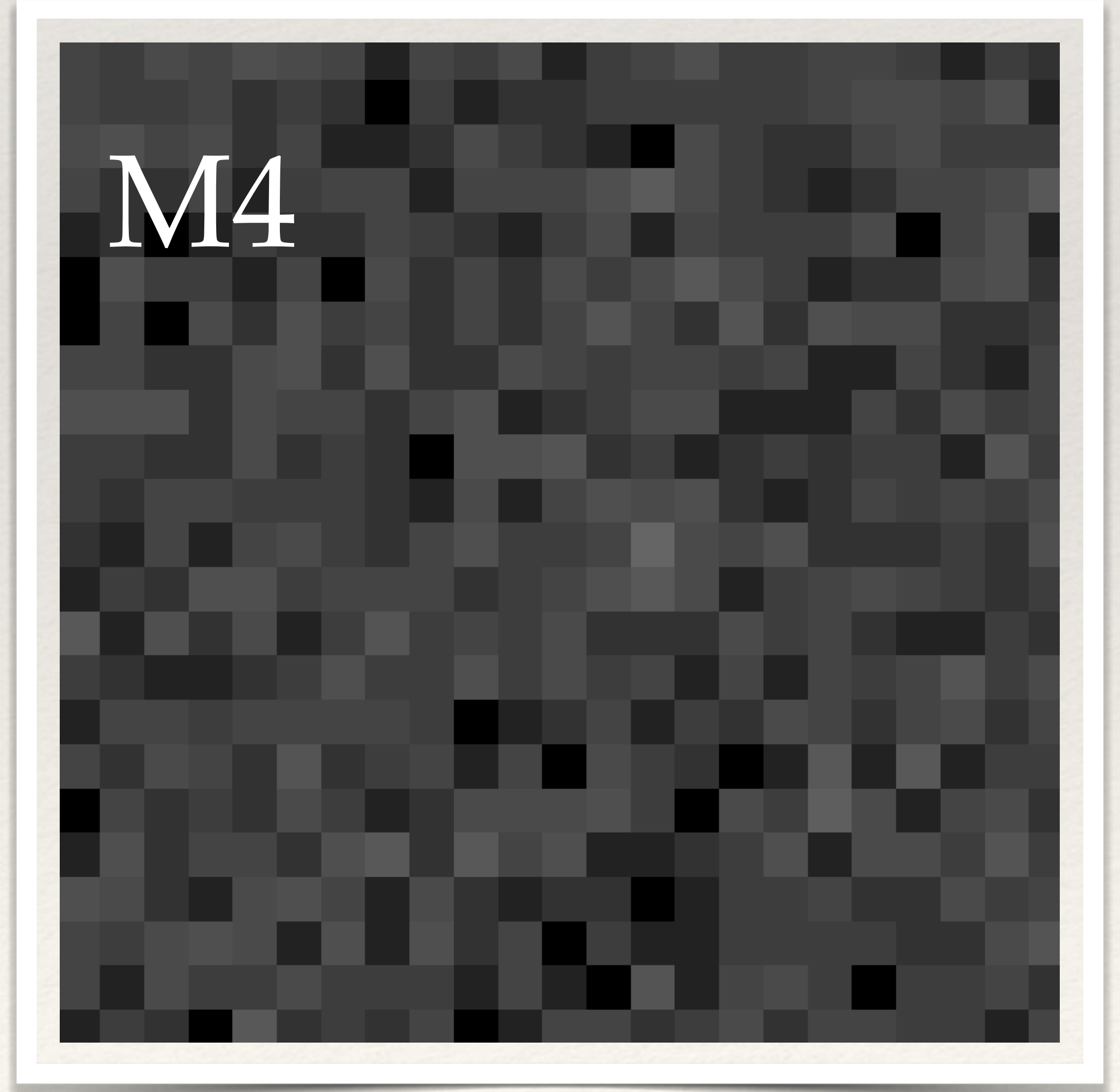

ROSAT (40 ksec)

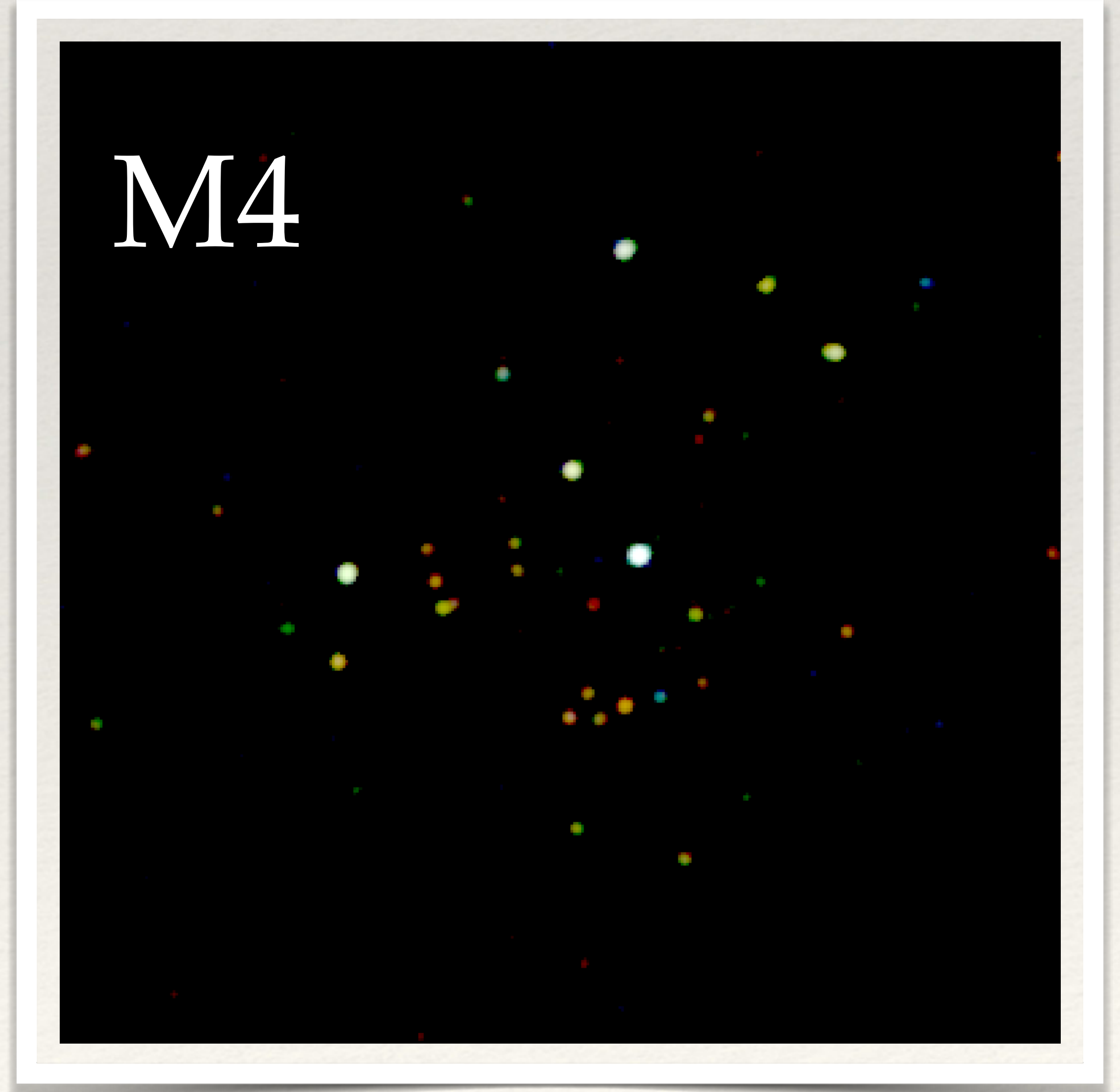

Chandra (120 ksec)

Chandra Observations Propel the Field Forward

- Differences in source populations were soon linked to internal dynamics in the clusters.
- The total number of X-ray sources in a cluster scales with the stellar encounter frequency (DP et al. 2003, Heinke et al. 2003, Gendre et al. 2003)
- With some knowledge gained, qLMXBs and some CVs could be separated from the rest of the population. CVs were ***finally*** shown to have a link to cluster dynamics, though not as strong a link as the LMXBs have.

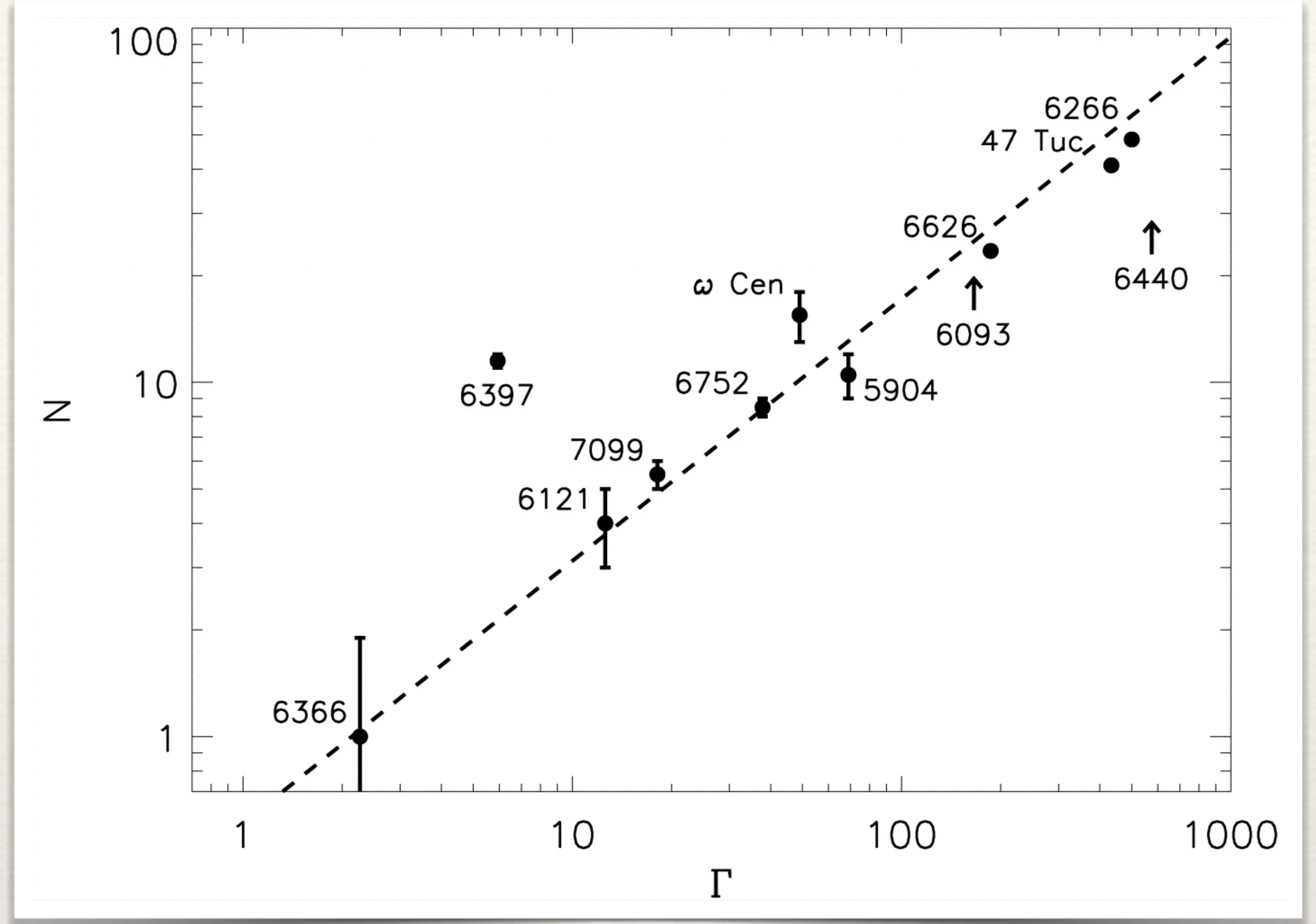

DP et al. (2003)

$$\Gamma = \int_0^{r_h} R\,dV$$

$$R \sim \rho^2/v$$

$$n = N/M$$

$$\gamma = \Gamma/M$$

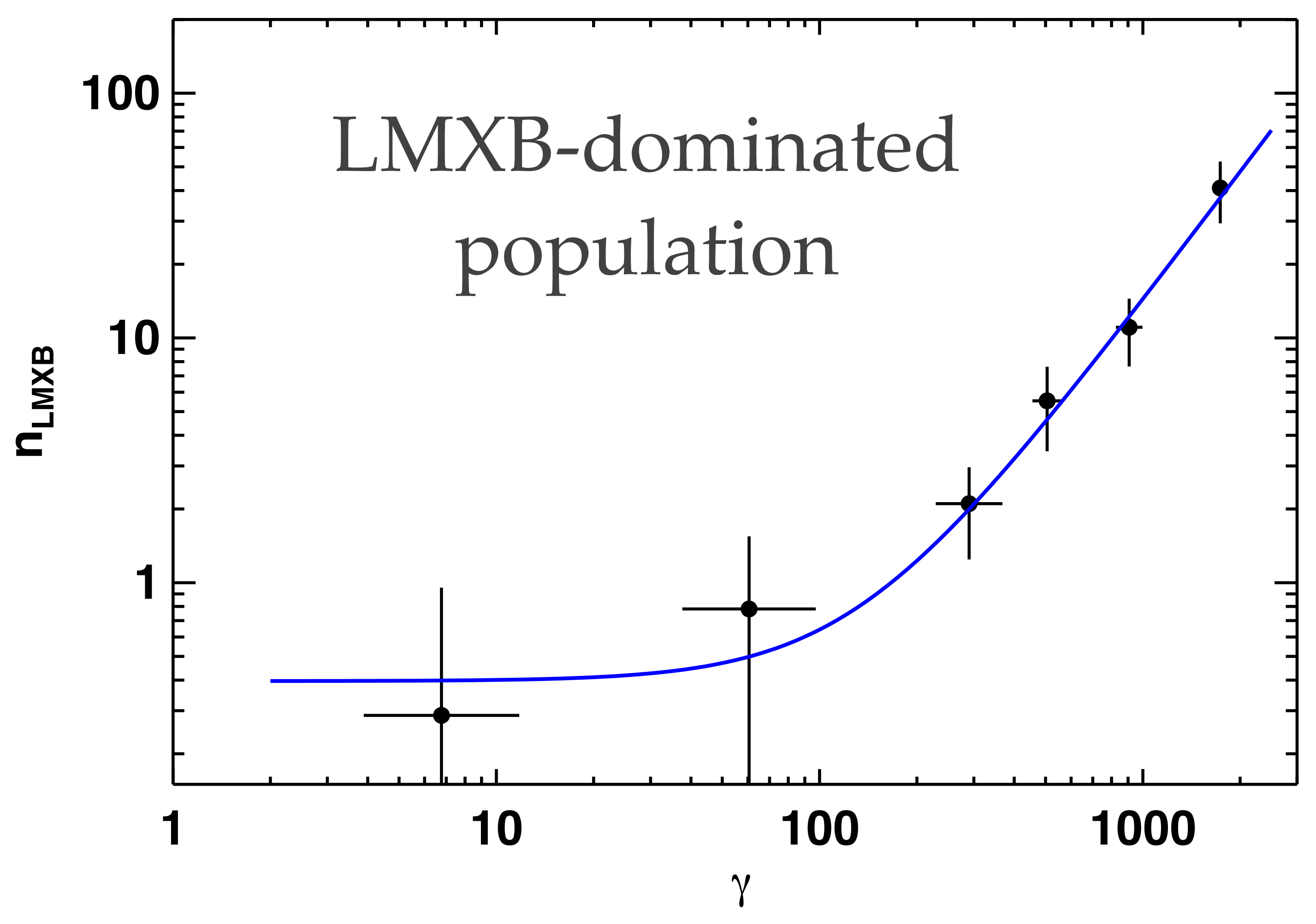

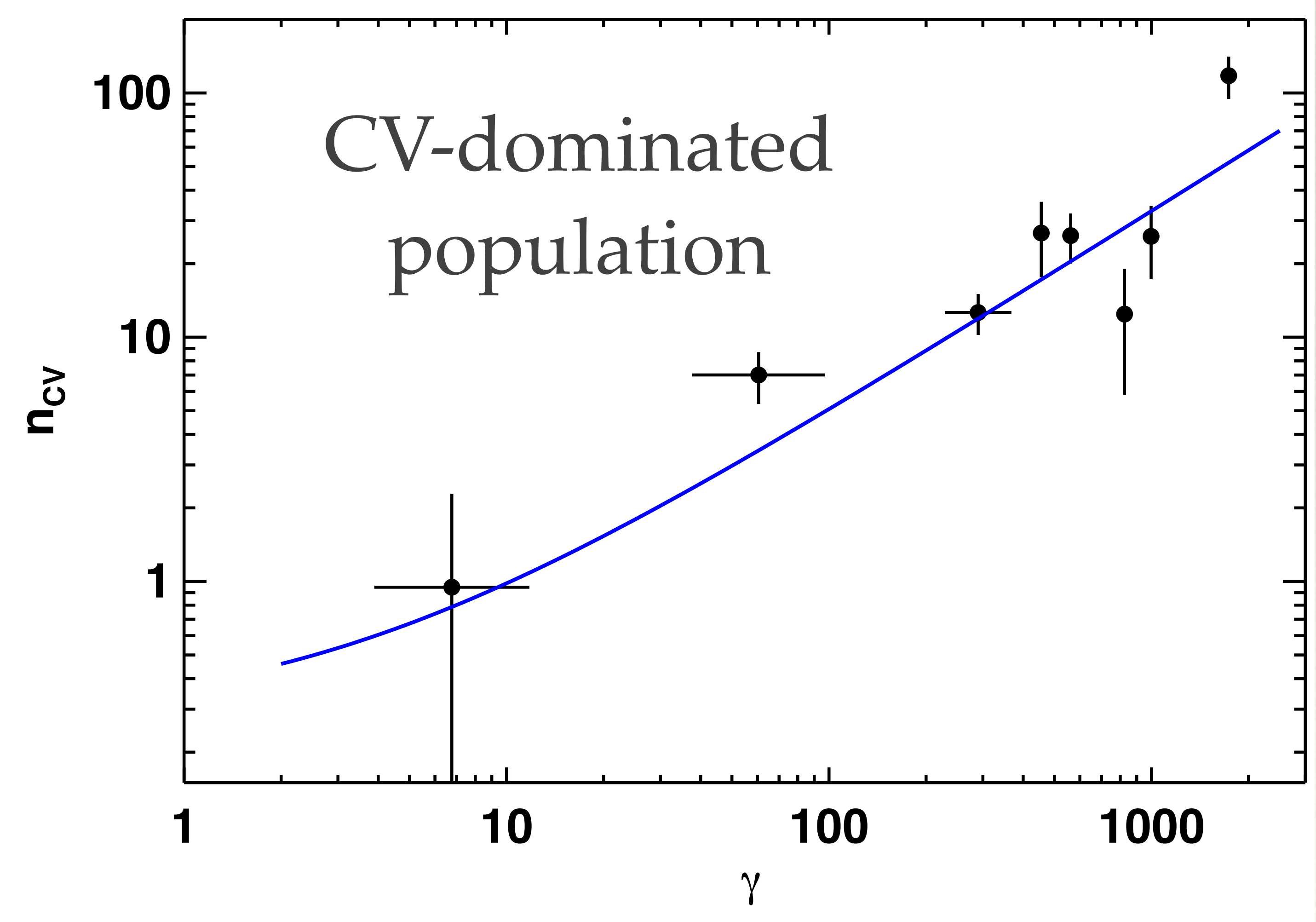

DP and Hut (2006)

X-rays Observations Probe Supernova Environments

- When the outgoing blast wave from a supernova (SN) runs into the circumstellar material (CSM) — which is formed by the wind(s) from the progenitor star — two shock fronts form, and both the shocked SN ejecta and CSM can emit X-rays.
- The X-ray luminosity is a function of the CSM density.
- The fast-moving SN shocks are effectively a time machine, encountering material shed earlier and earlier in the life of the pre-supernova star.
- The X-ray light curve gives us a picture of thousands of years of the mass-loss history of the SN progenitor.

Credit: NASA/CXC/A. Hobart

The Circumstellar Medium Is Not Uniform

- Major issue in supernova (SN) research is how massive stars that begin with ~70% hydrogen are nearly or completely devoid of H when they explode as Type Ic, Ib, Ibn, or IIb SNe.
- SN 2001em (Ic) found to have strong radio (Stockdale et al. 2004) and X-ray (DP & Lewin 2004) emission years after explosion. Optical spectrum showed strong Hα (Soderberg et al. 2004). Explained as SN shock catching up to previously expelled H envelope at 7×10^{16} cm and undergoing strong interaction (Chugai & Chevalier 2006).

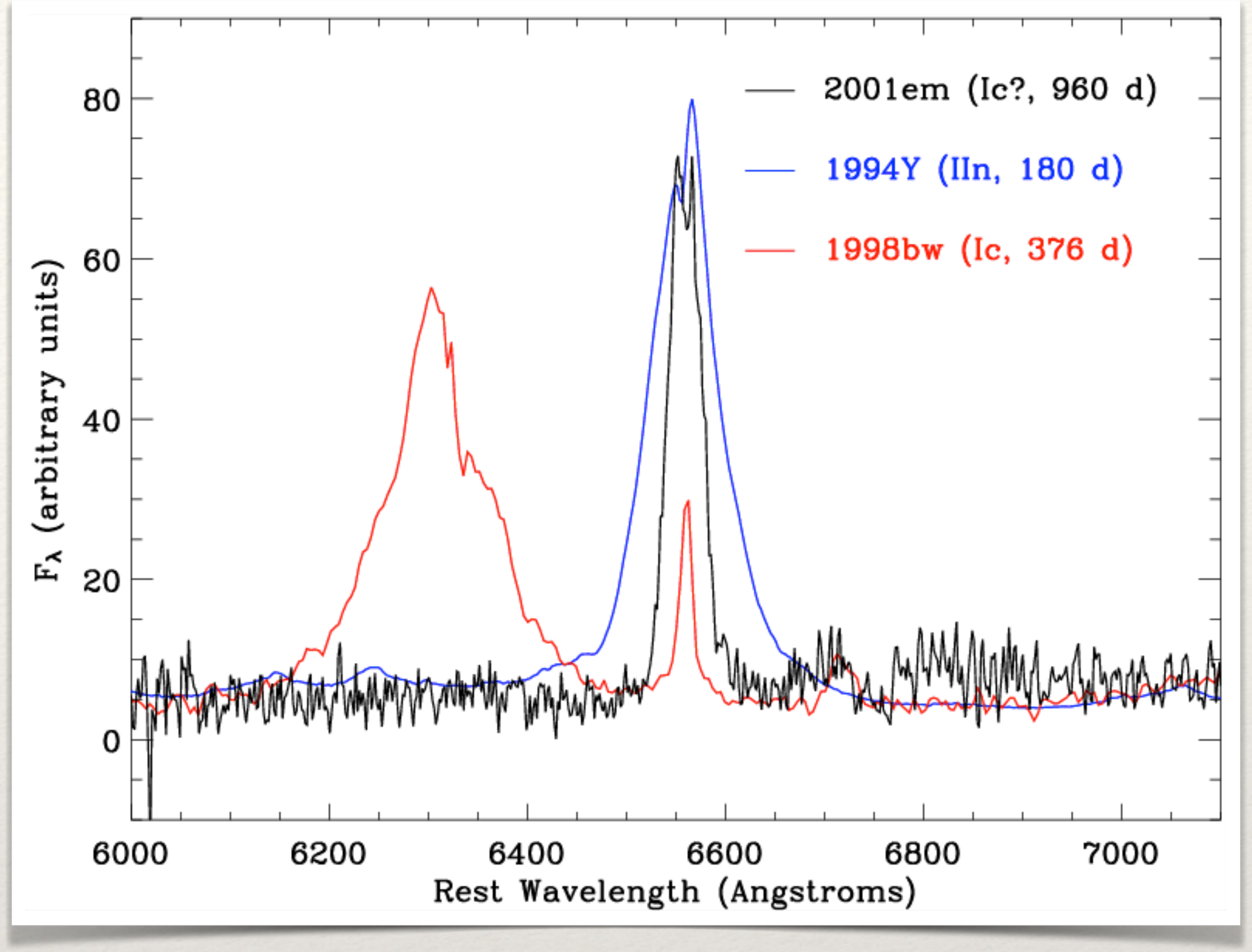

Soderberg et al. 2004

- SN 2006jc (Ib) showed 5× rise X-rays ~100 days after explosion, interpreted as dense shell at 10^{16} cm (Immler et al. 2008).
- SN 2014C (Ib) showed strong Hα 127 days after explosion, along with X-ray, radio, and IR emission (Milisavljevic et al. 2015; Tinyanont et al. 2016; Thomas et al. 2022)
- SN 2004dk (Ib) showed strong Hα, X-rays, and radio 10–15 years after explosion (Vinko et al. 2017; DP et al. 2019)

see poster by V. Dwarkadas

The Resolution of *Chandra* Is Crucial

- CSM interaction is the source of (almost) all X-ray emission from young SNe.
- Measuring CSM properties provides vital information on the mass-loss history of the progenitor.
- *Chandra*, *XMM*, and *Swift* have all contributed to substantial progress in understanding CSM interaction.
- SNe have a bad habit of happening in galaxies. Galaxies have XRBs.
- Chandra observations are necessary to isolate SN X-ray emission from other sources.

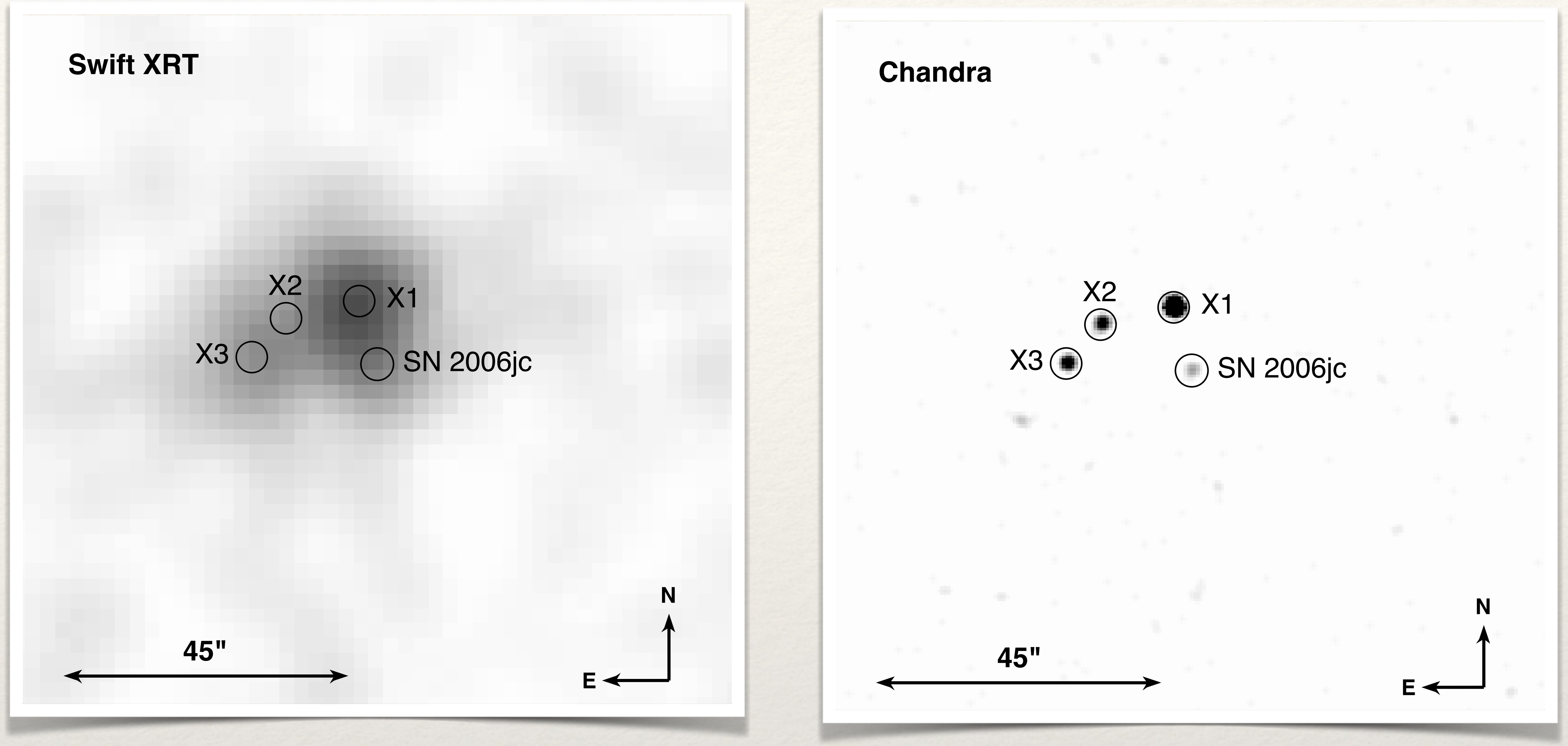

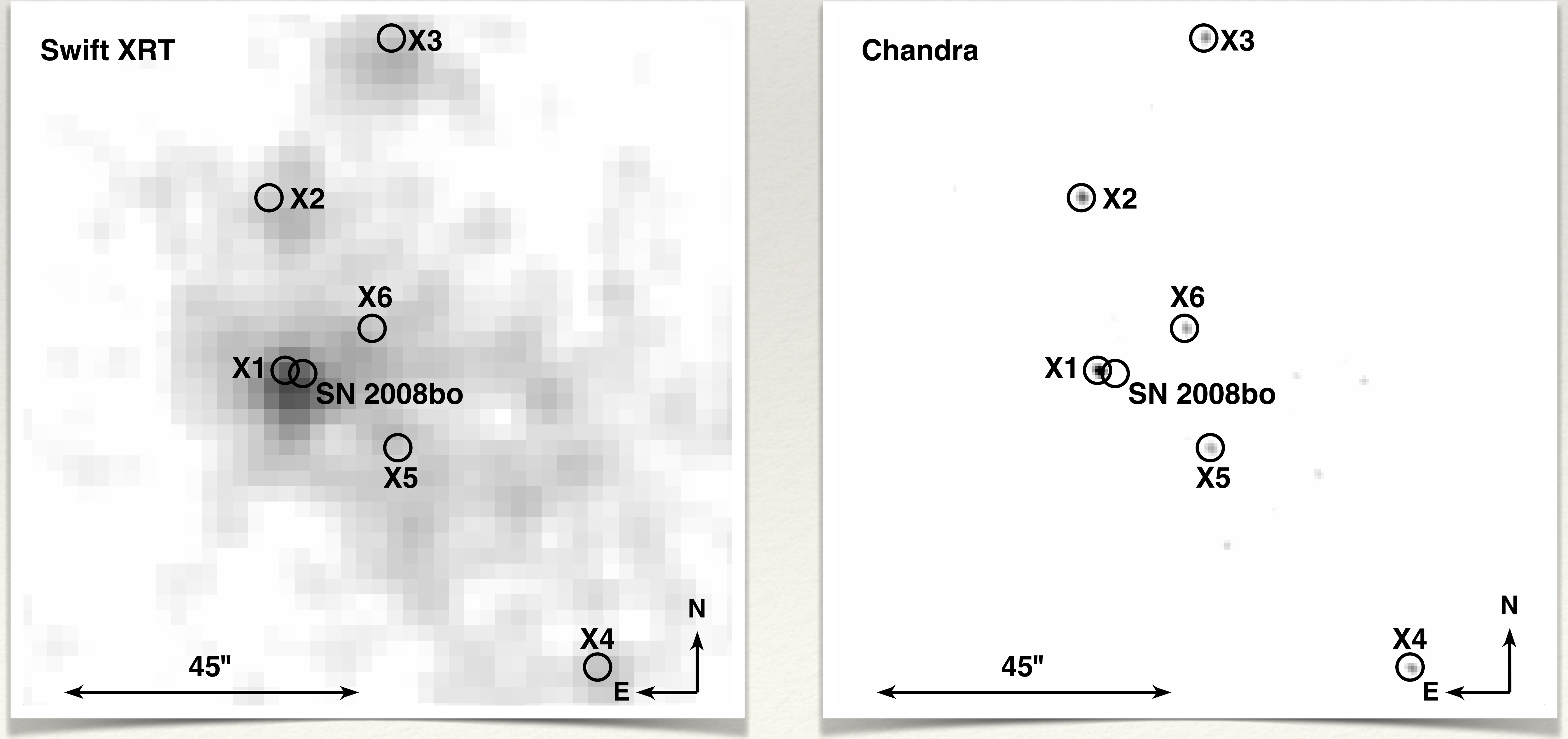

Lensed Quasars: The Mystery of Flux Ratio Anomalies

- Flux ratio anomalies in lensed quasars were known in the optical for decades and thought to be due to small scale structure in lensing galaxy. Arguments were put forth for two leading candidates
- Milli-lensing: dark matter condensations of $10^4 - 10^6\ M_\odot$ (Wambsganss & Paczyński 1992; Witt et al. 1995; Mao & Schneider 1998; Metcalf & Madau 2001; Dalal & Kochanek 2002; Chiba 2002)
- Micro-lensing: stars in the lensing galaxy (Witt et al. 1995; Schechter & Wambsganss 2002)

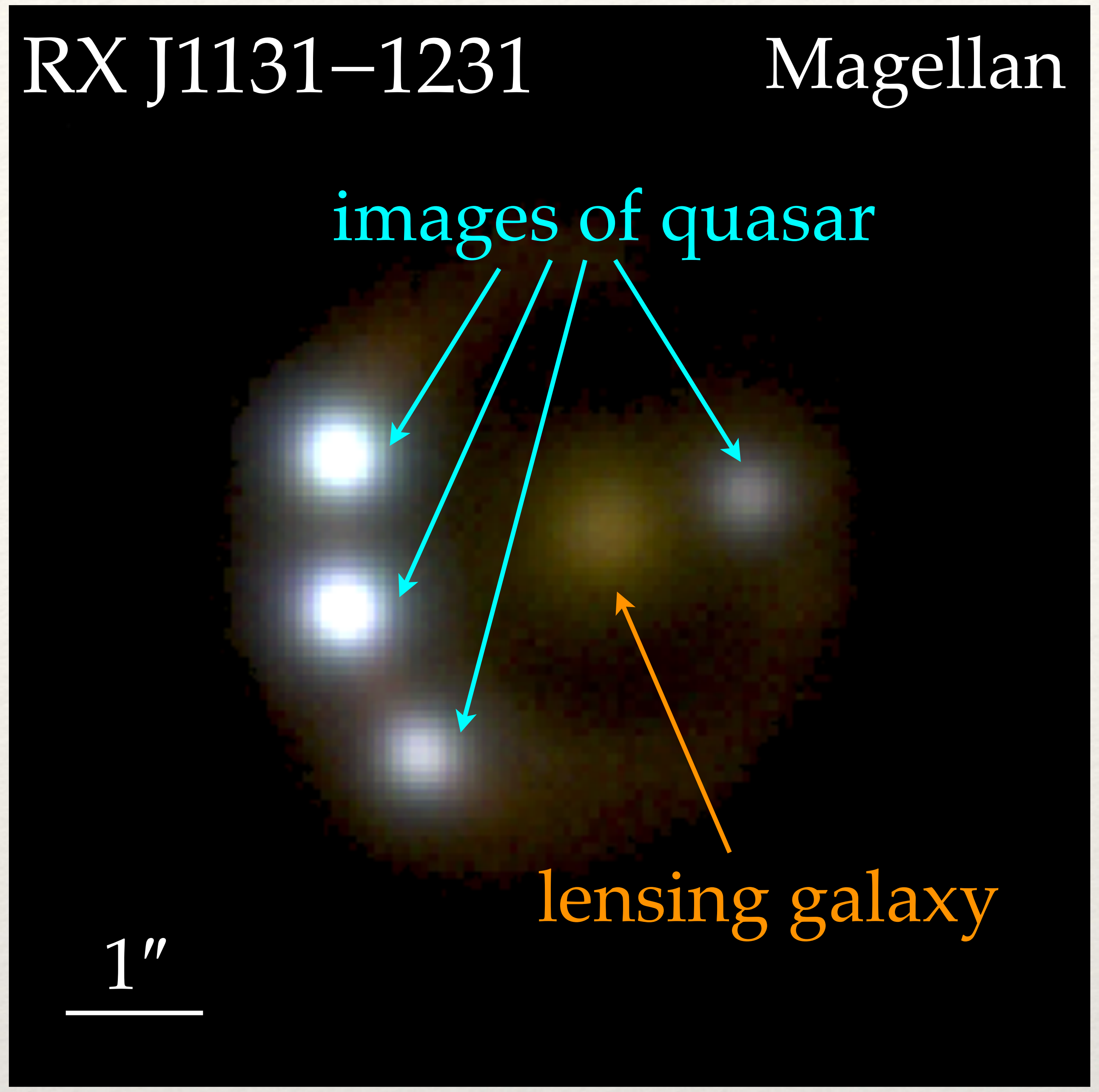

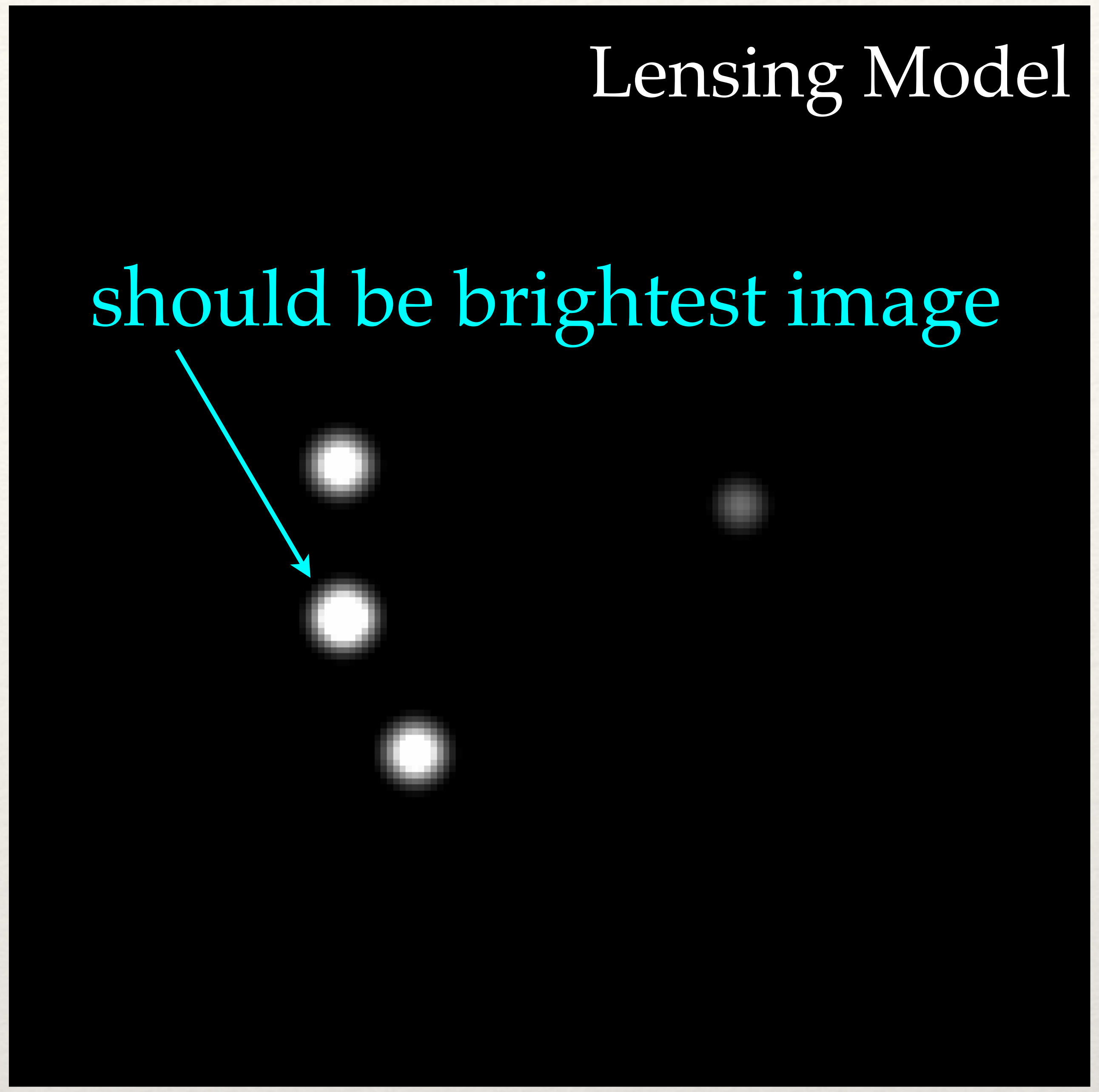

Blackburne, DP, & Rappaport 2006

Chandra Observations Solve the Mystery

- *Chandra* observations established that stronger X-ray anomalies are nearly universal, indicating micro-lensing is the cause of the anomalies (DP et al. 2007).
- This allowed micro-lensing to be used as a tool to study both the sources (quasars) and the lenses (elliptical galaxies) on scales of micro-arseconds.
- Magnitude of micro-lensing effects probes source size (quasar structure).
- Frequency of micro-lensing effects probes lensing galaxy contents.

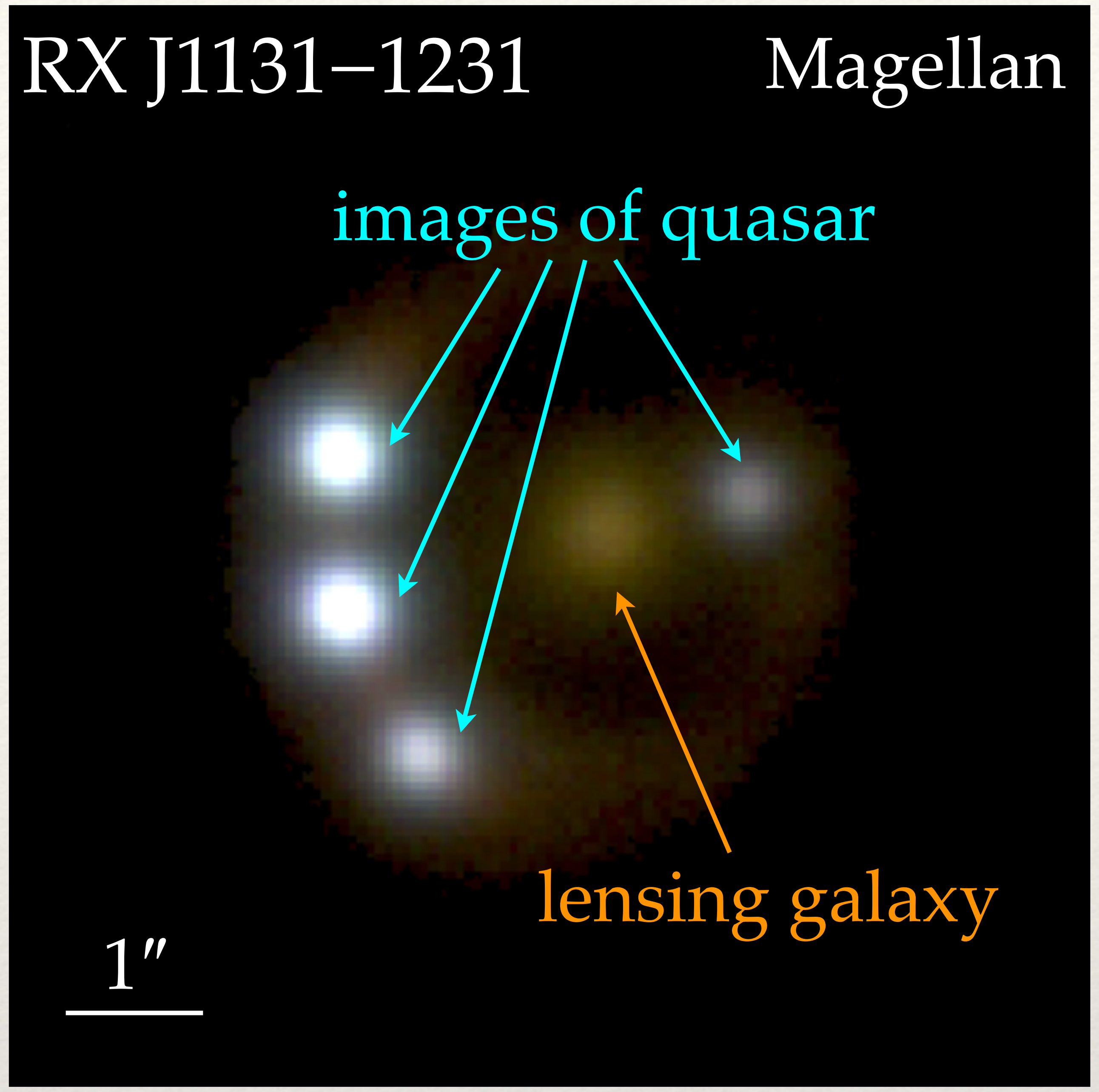

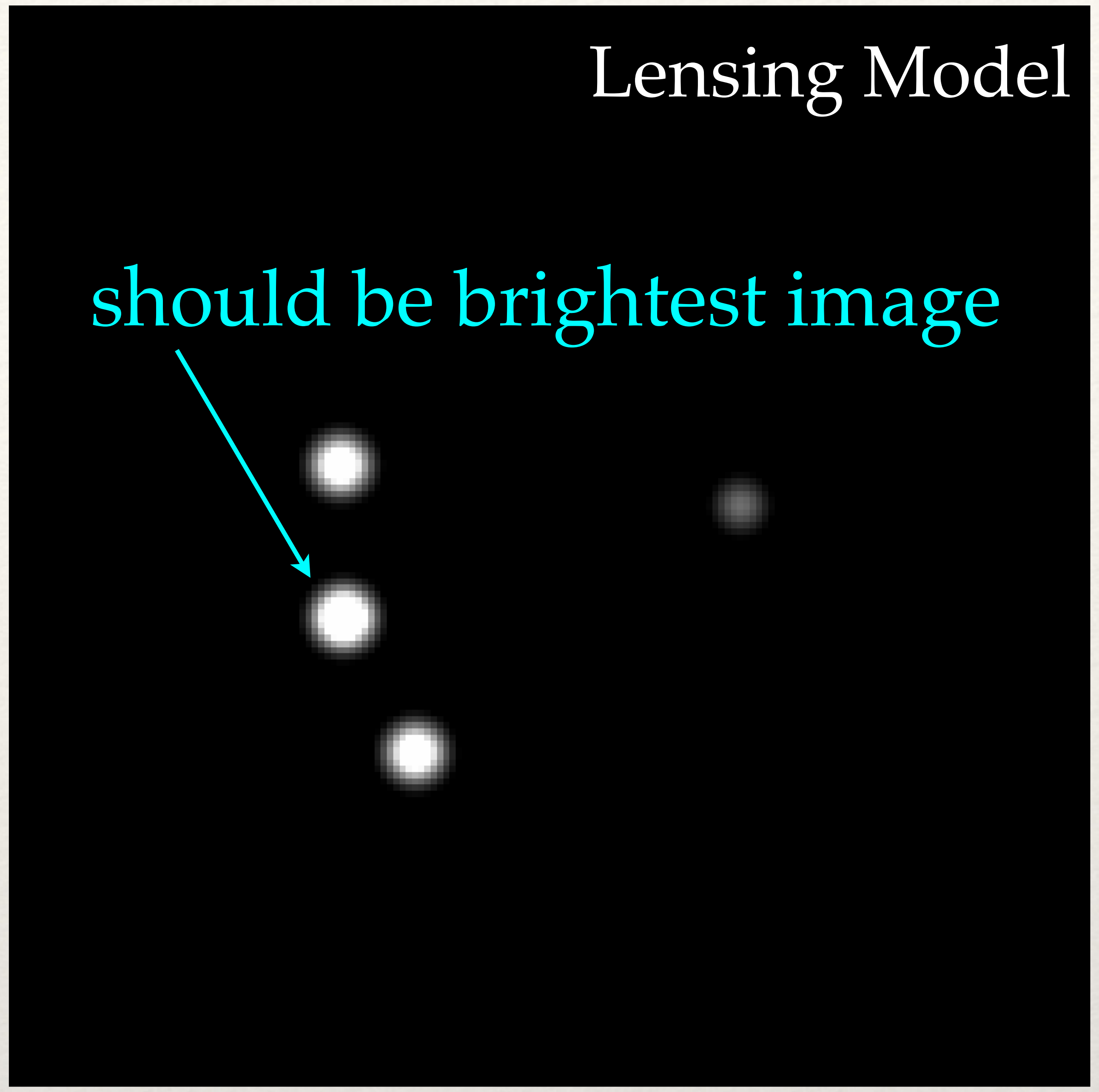

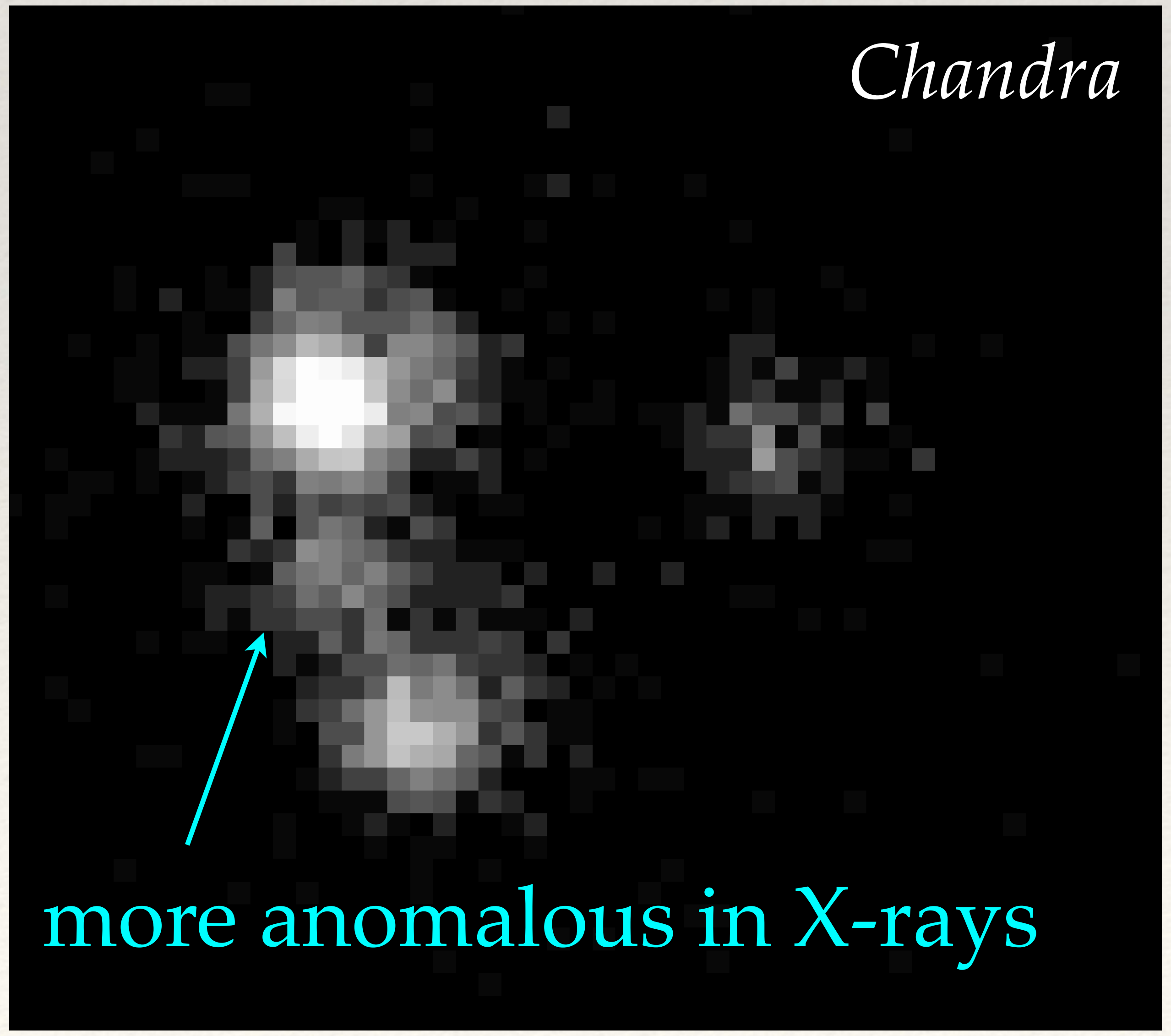

Blackburne, DP, & Rappaport 2006

The Anomalies Are Now a **Powerful** Tool

Lensing galaxy: the probability of strong micro-lensing effects is a non-monotonic function of stellar density.

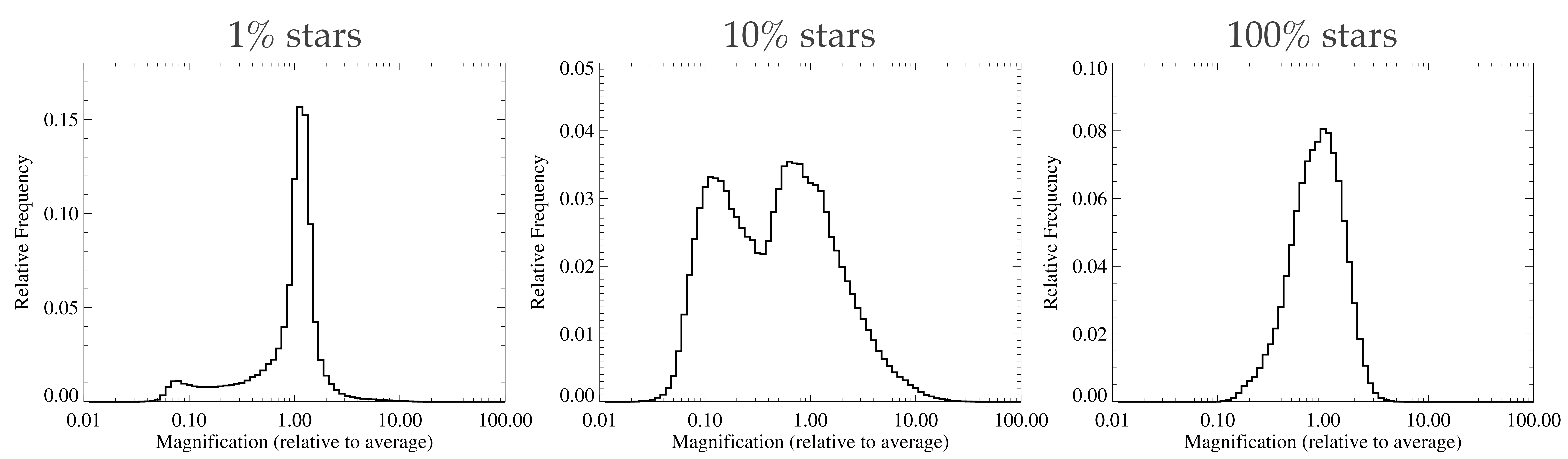

X-rays give clean signal of micro-lensing effects; bayesian analysis of *Chandra* fluxes gives likelihood of stellar fraction.

The Anomalies Are Now a **Powerful** Tool

Lensing galaxy: ensemble average stellar fraction is ~7% at typical impact parameter of 7 kpc.

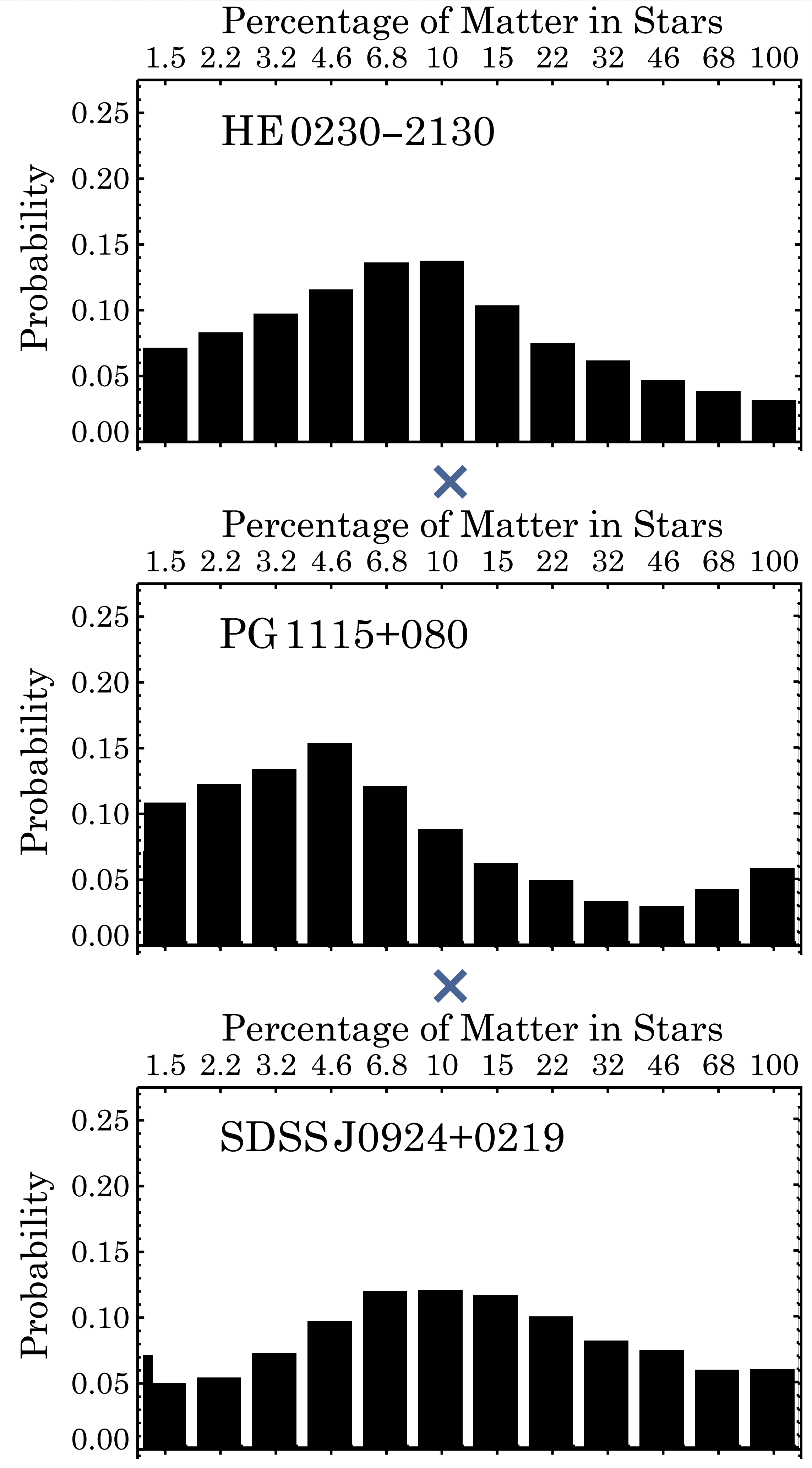

=

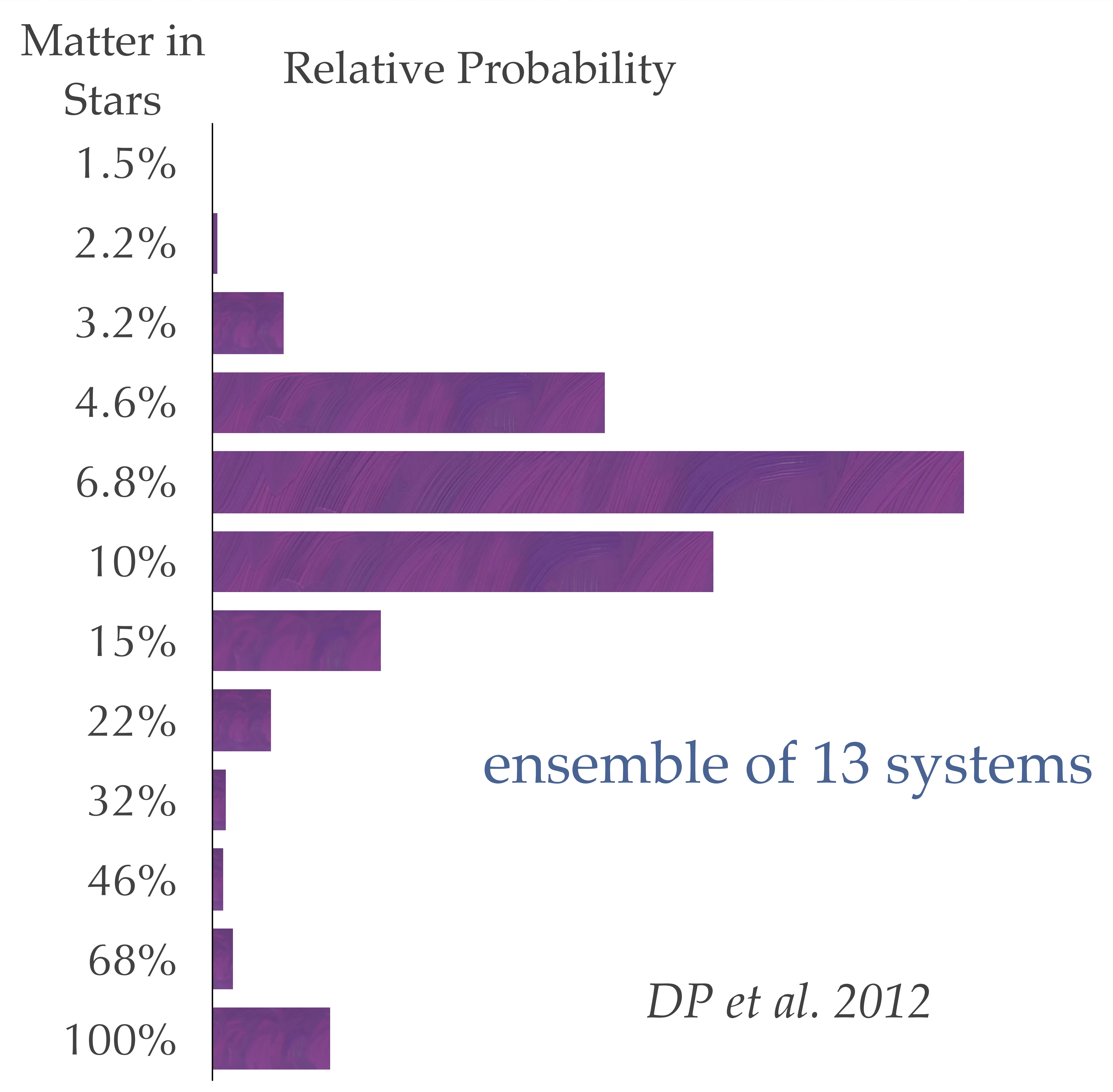

The Anomalies Are Now a **Powerful** Tool

Lensing galaxy: *Chandra* data determine stellar *M*/*L* via Fundamental Plane.

- Overall mass density of lensing galaxy is known from macro-lensing.
- *Chandra* gives level of micro-lensing → mass in individual stars, including stellar remnants, brown dwarfs, and red dwarfs too faint to produce photometric or spectroscopic signatures.
- We assess stellar *M*/*L* via a calibration factor $\mathcal{F}$ that multiplies the stellar mass fundamental plane.

$$0.77 < \mathcal{F} < 2.10$$

uncertainty dominated by small sample size.

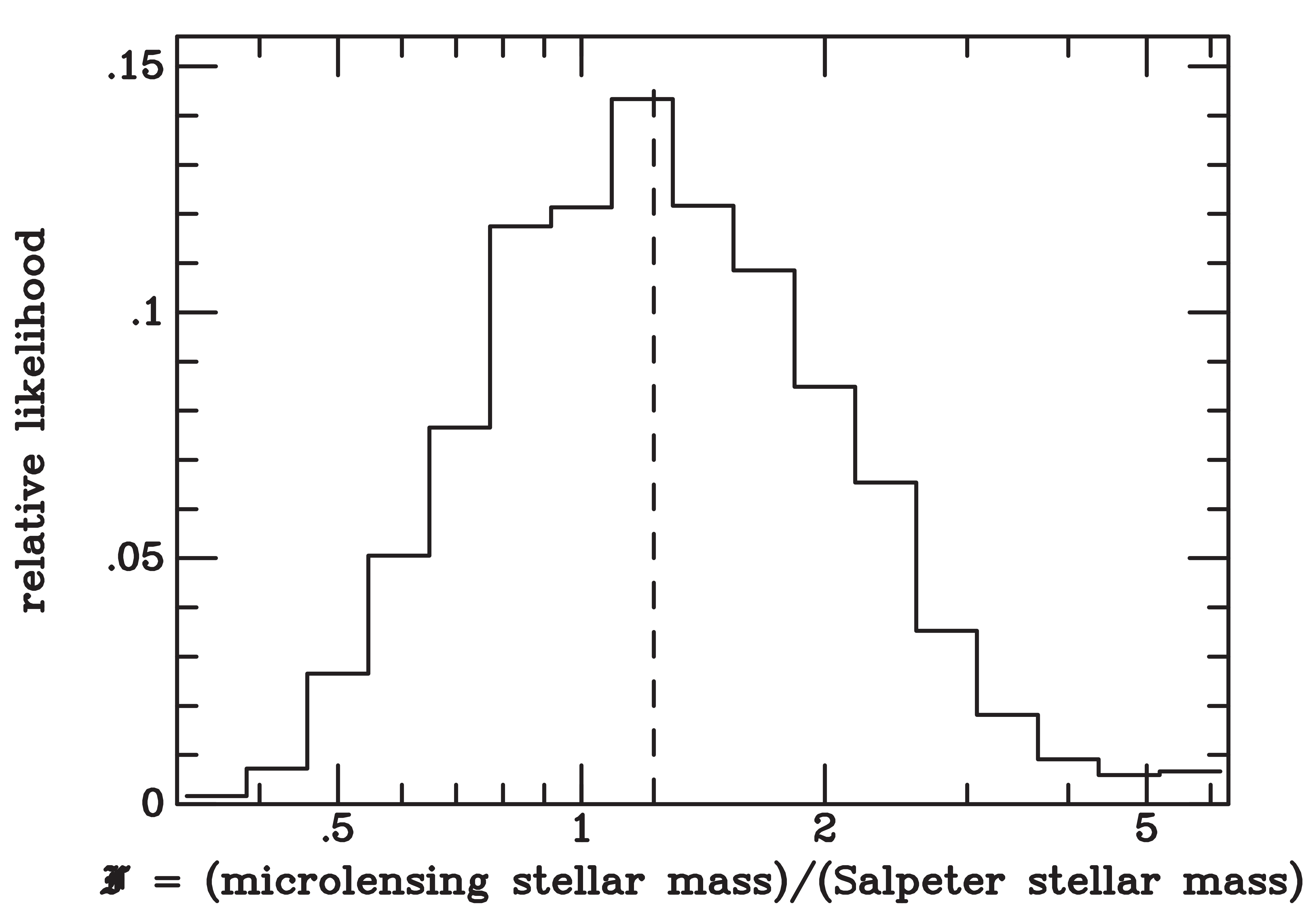

Schechter, DP, et al. 2014

The Anomalies Are Now a **Powerful** Tool

Lensing galaxy: *Chandra* data constrain mass of dark halo in MaCHOs to ≲10%.

- Previous assumption: dark halo component is smooth → halo particles of at most planetary mass (depends on X-ray size of quasar)
- Instead, take stellar surface mass density to be known and let the factor $\mathscr{F}$ represent the fraction of the dark halo in Massive Compact Halo Objects (MaCHOs), which includes ~20 $M_\odot$ black holes.

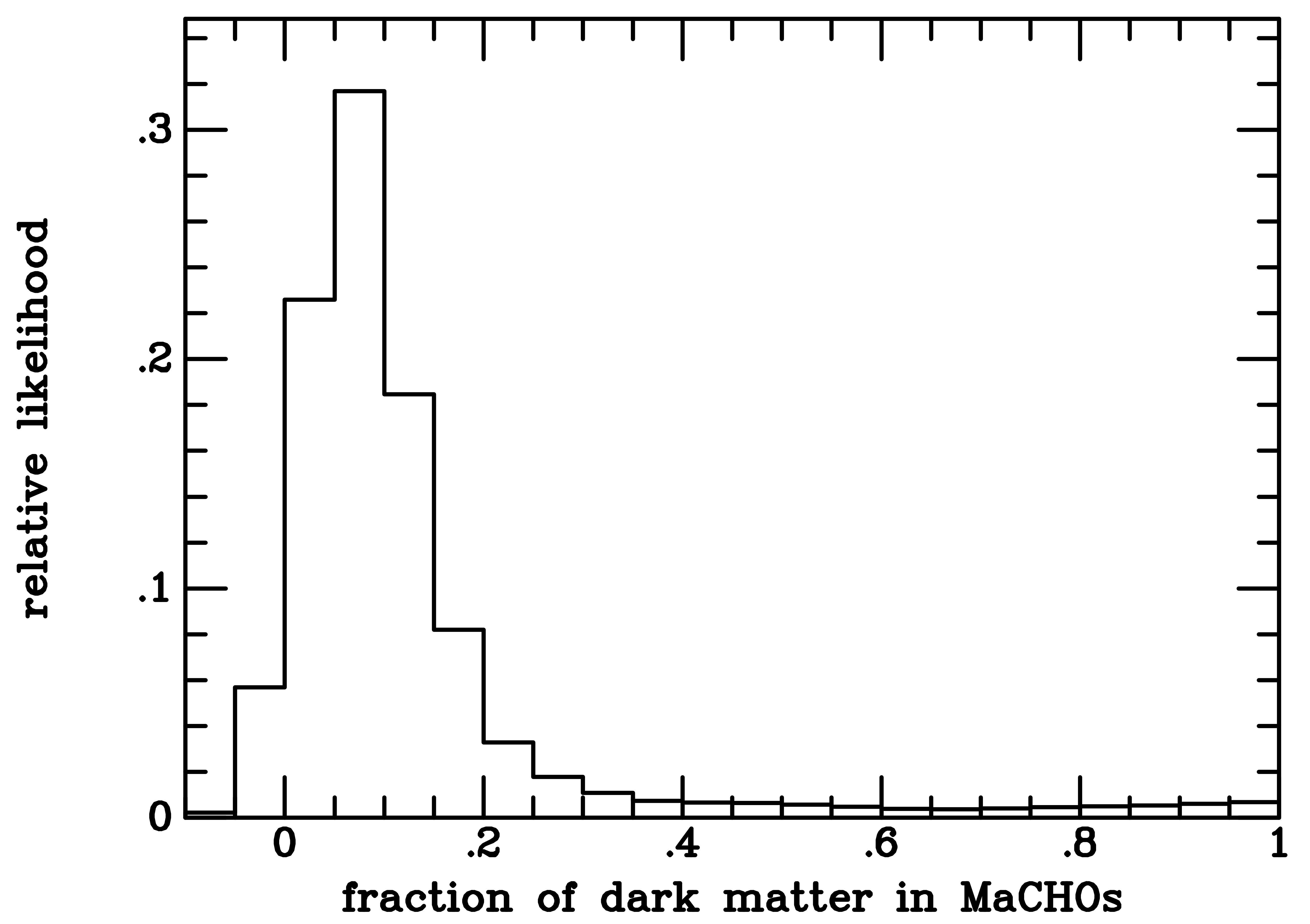

Schechter 2018

See also Mediavilla et al. (2009)

The Anomalies Are Now a **Powerful** Tool

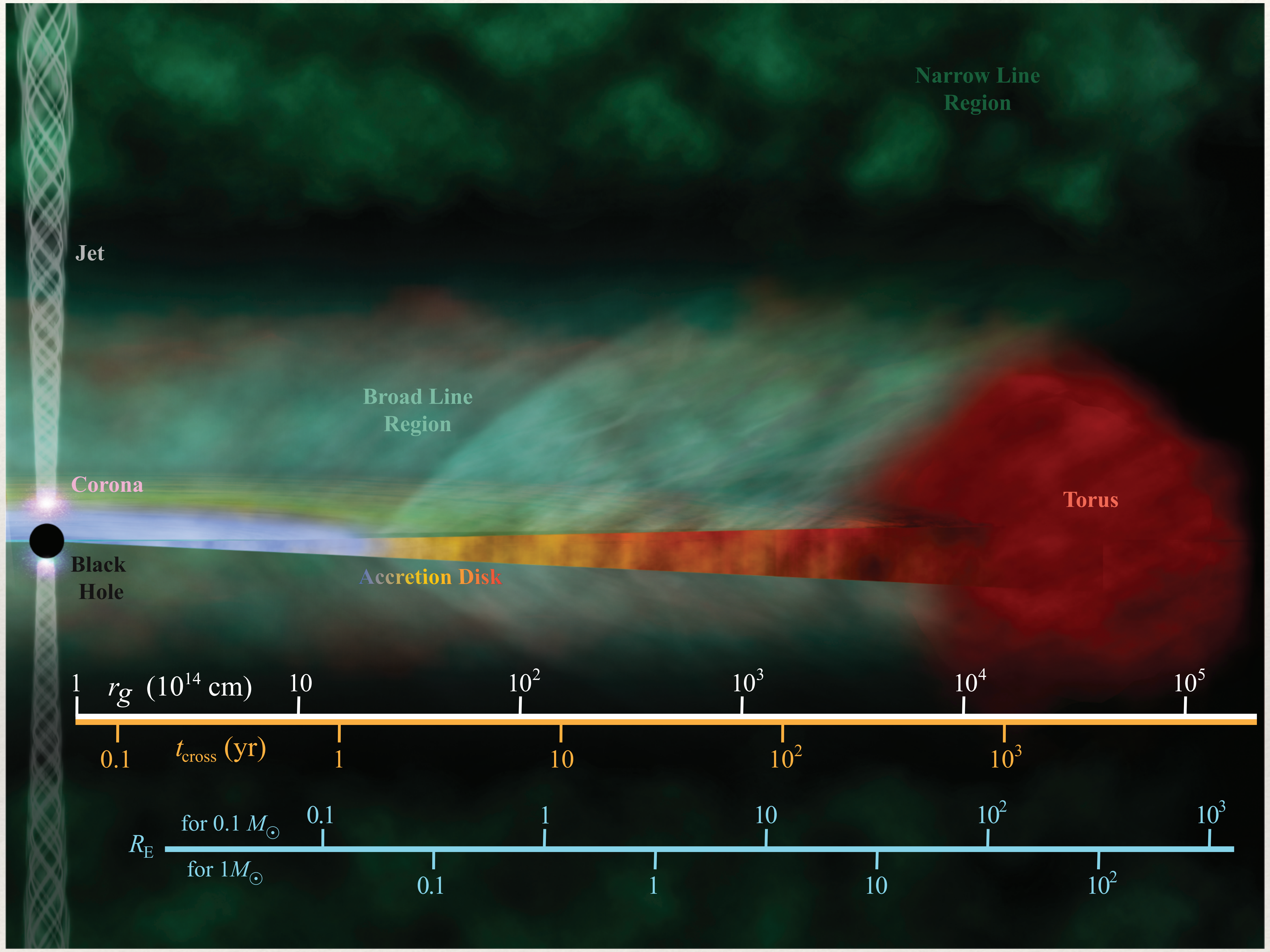

Schematic view of the structure of a quasar with the main regions that can be probed by micro-lensing color-coded as follows, starting from the smallest/ innermost (left to right): X-ray corona (purple), accretion disc (blue to red), Broad Line Region (lighter green), dust torus (red), and Narrow Line Emission (darker green). For completeness, the black hole and the jet are also shown.

(from Varnardos, Sluse, DP, et al. 2024)

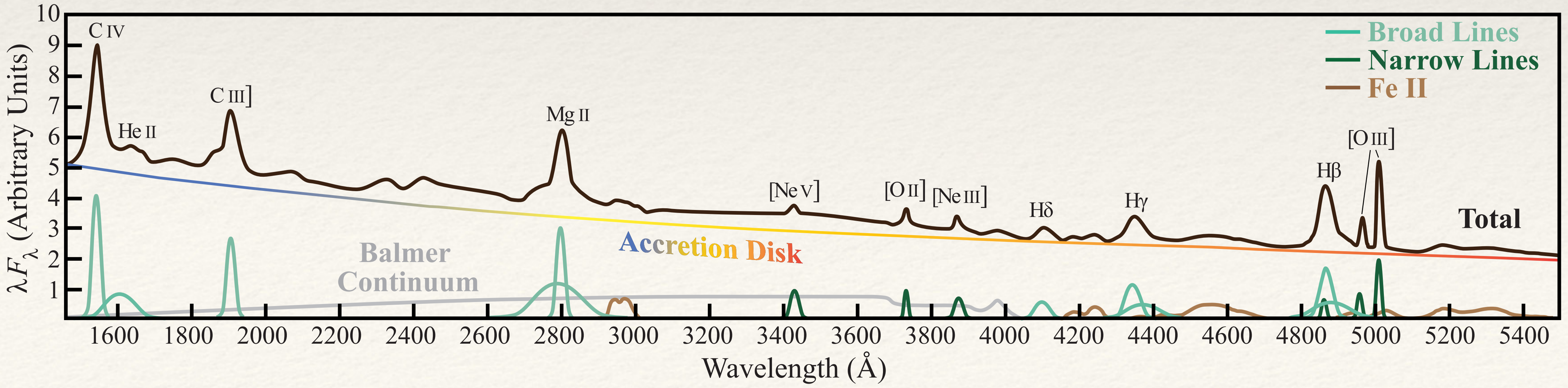

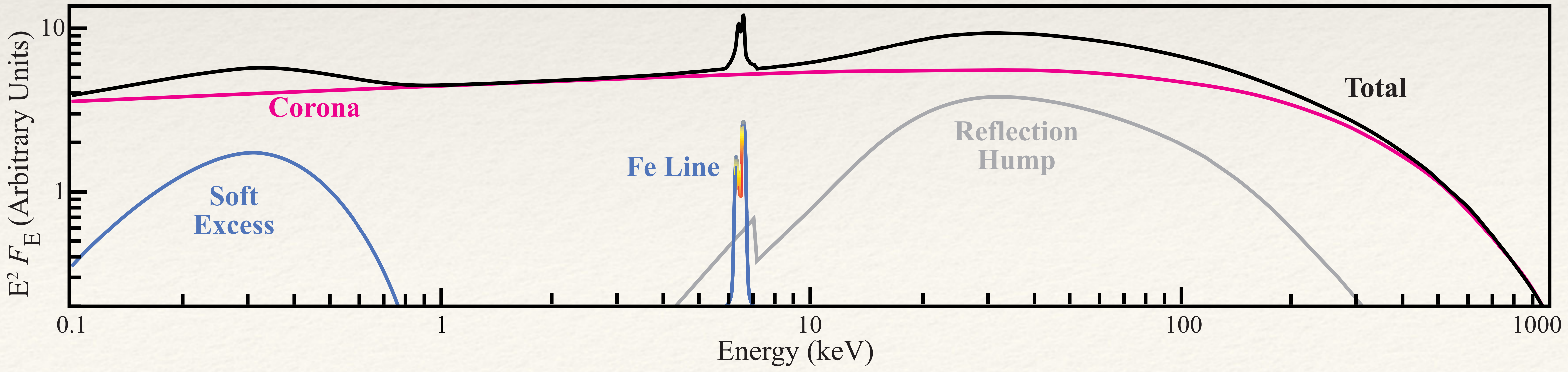

The Anomalies Are Now a **Powerful** Tool

Quasar Structure: micro-lensing has ruled out certain corona geometries and established that the corona must be compact.

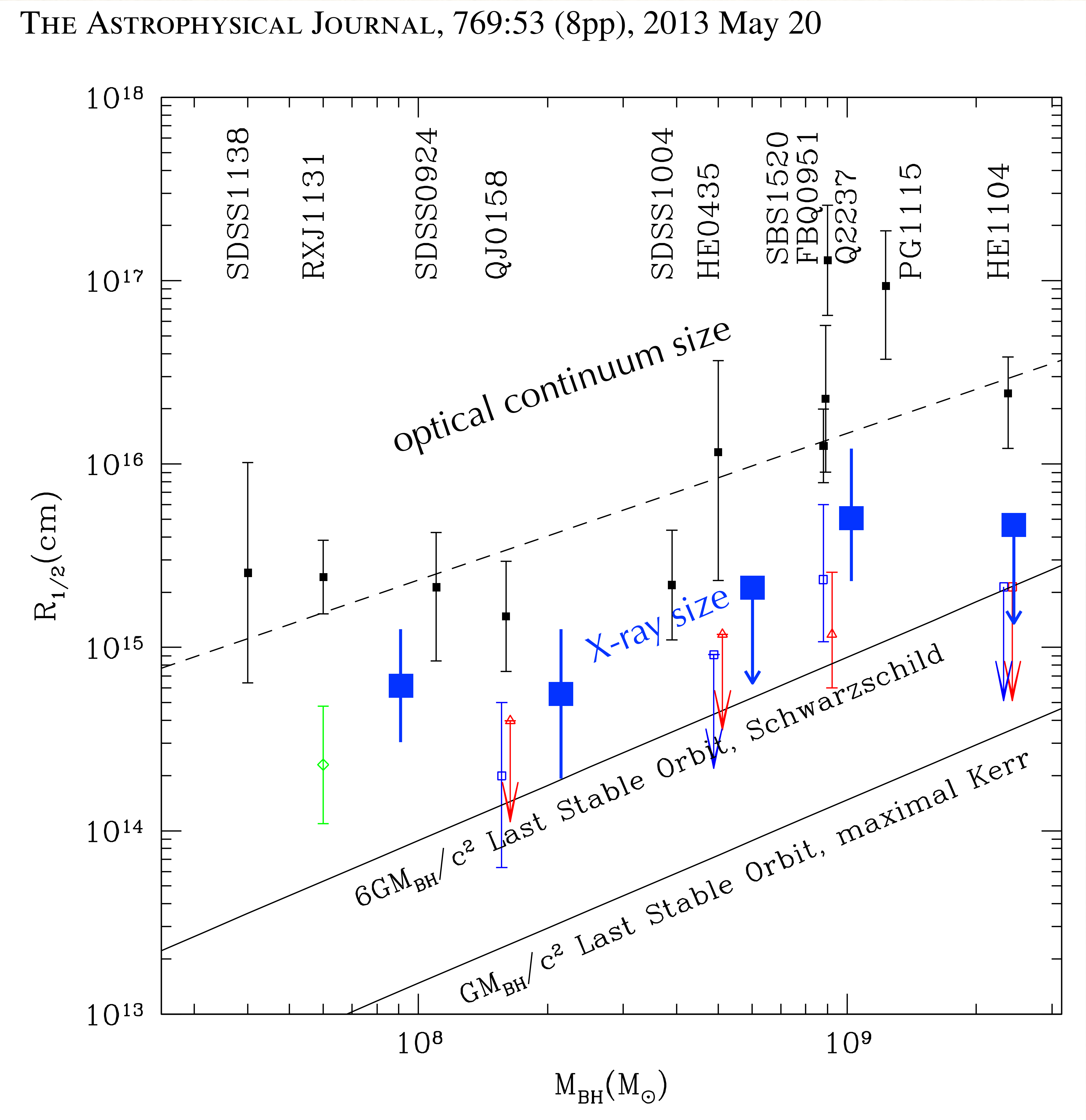

Mosquera et al. 2013

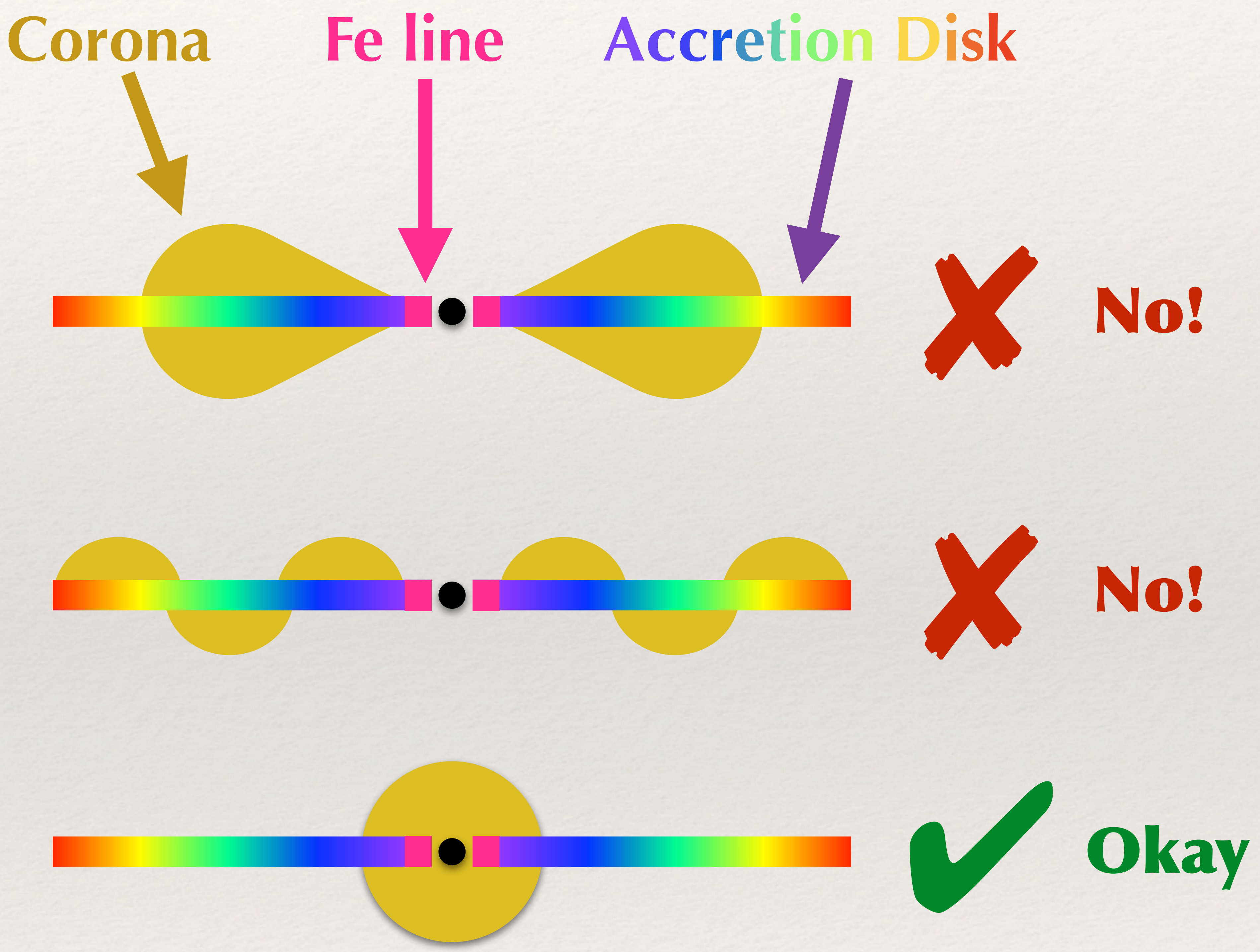

See also DP et al (2007); Chartas et al. (2009); Dai et al. (2010); Morgan et al. (2010, 2012); Blackburne et al. (2011a)

The Anomalies Are Now a **Powerful** Tool

Quasar Structure: optical disk is 3 – 30× larger than standard thin-disk theory.

Diminished micro-lensing in optical

Estimate size of optical disk necessary to give that much less variability

Ensemble average

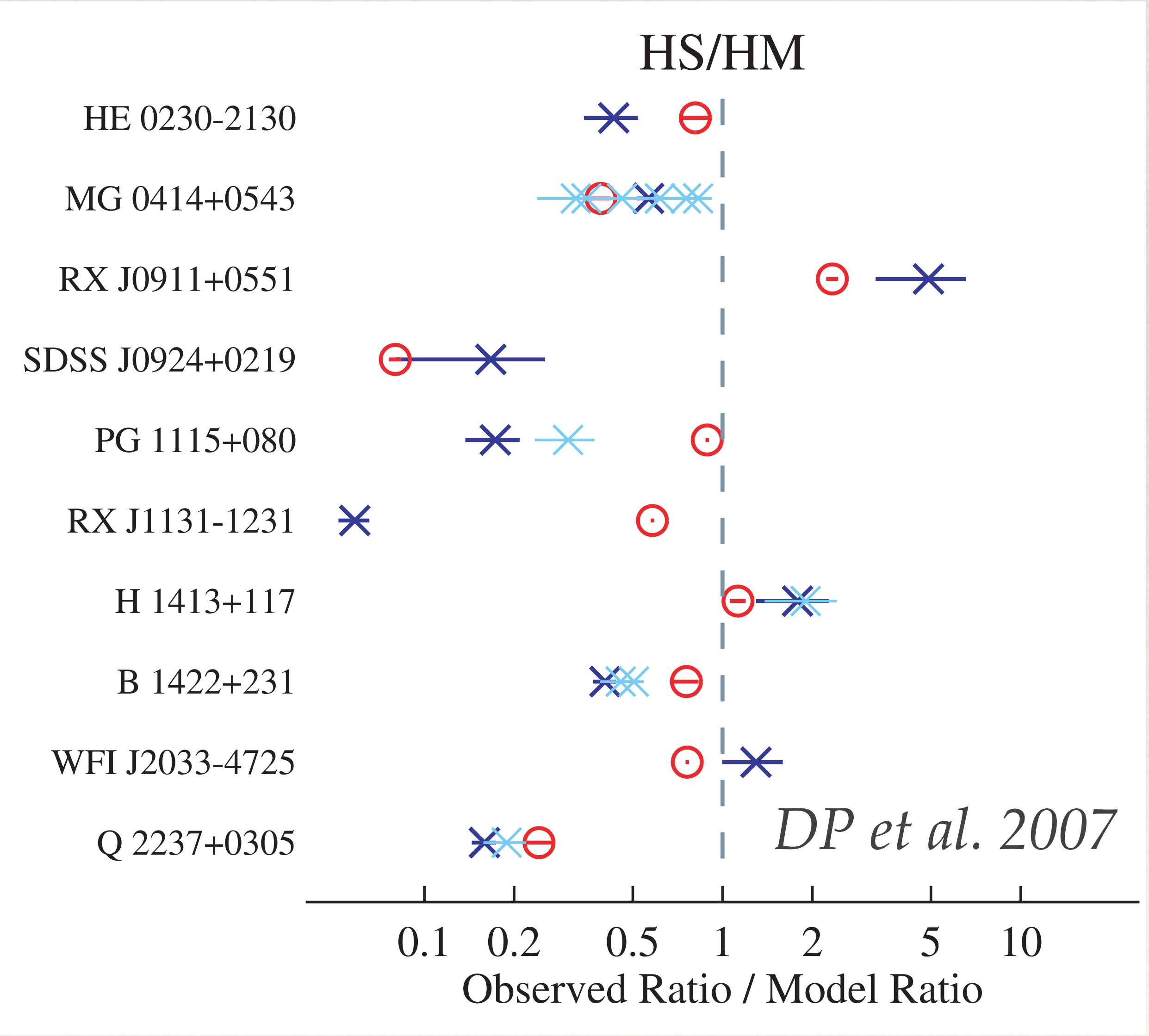

Individual systems

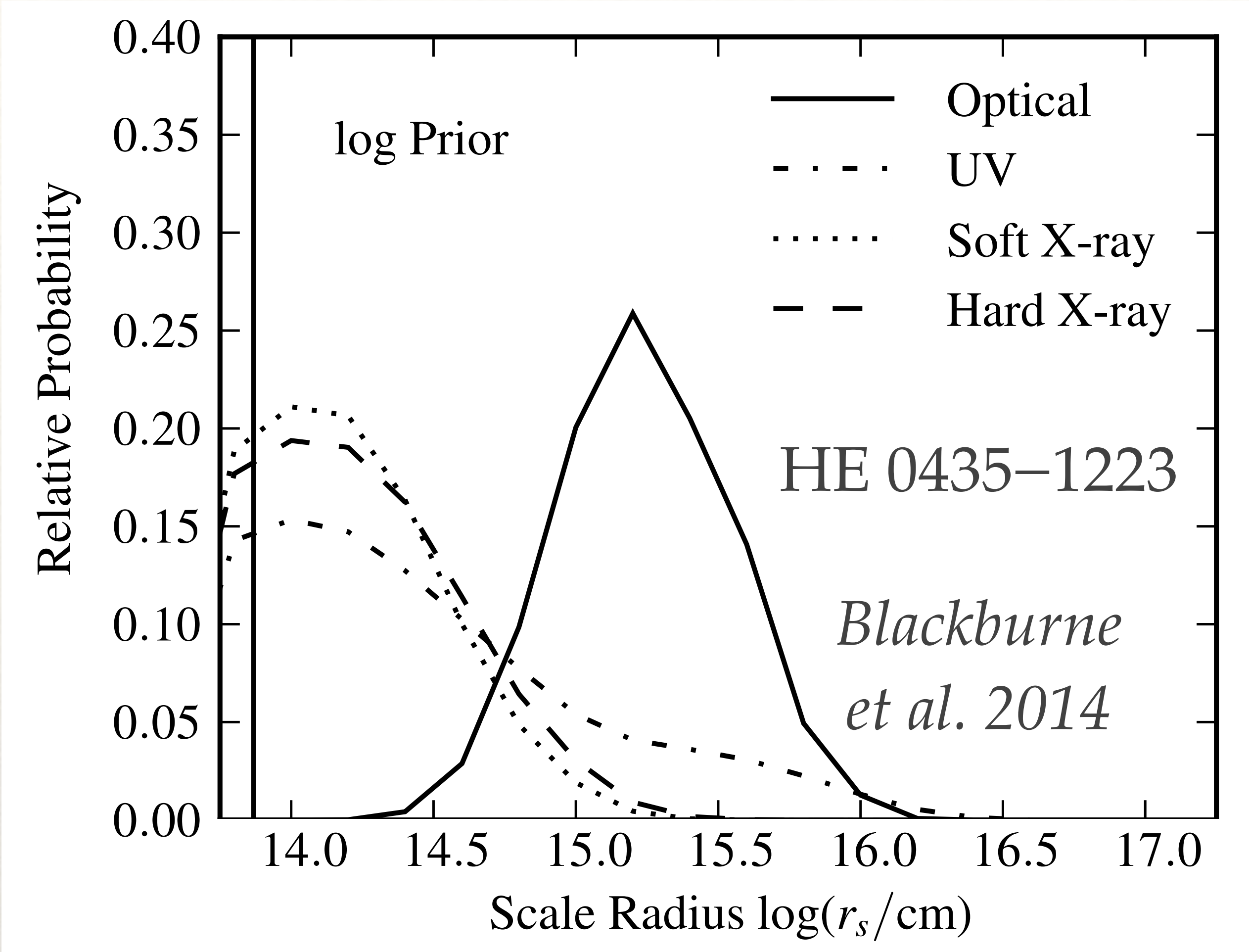

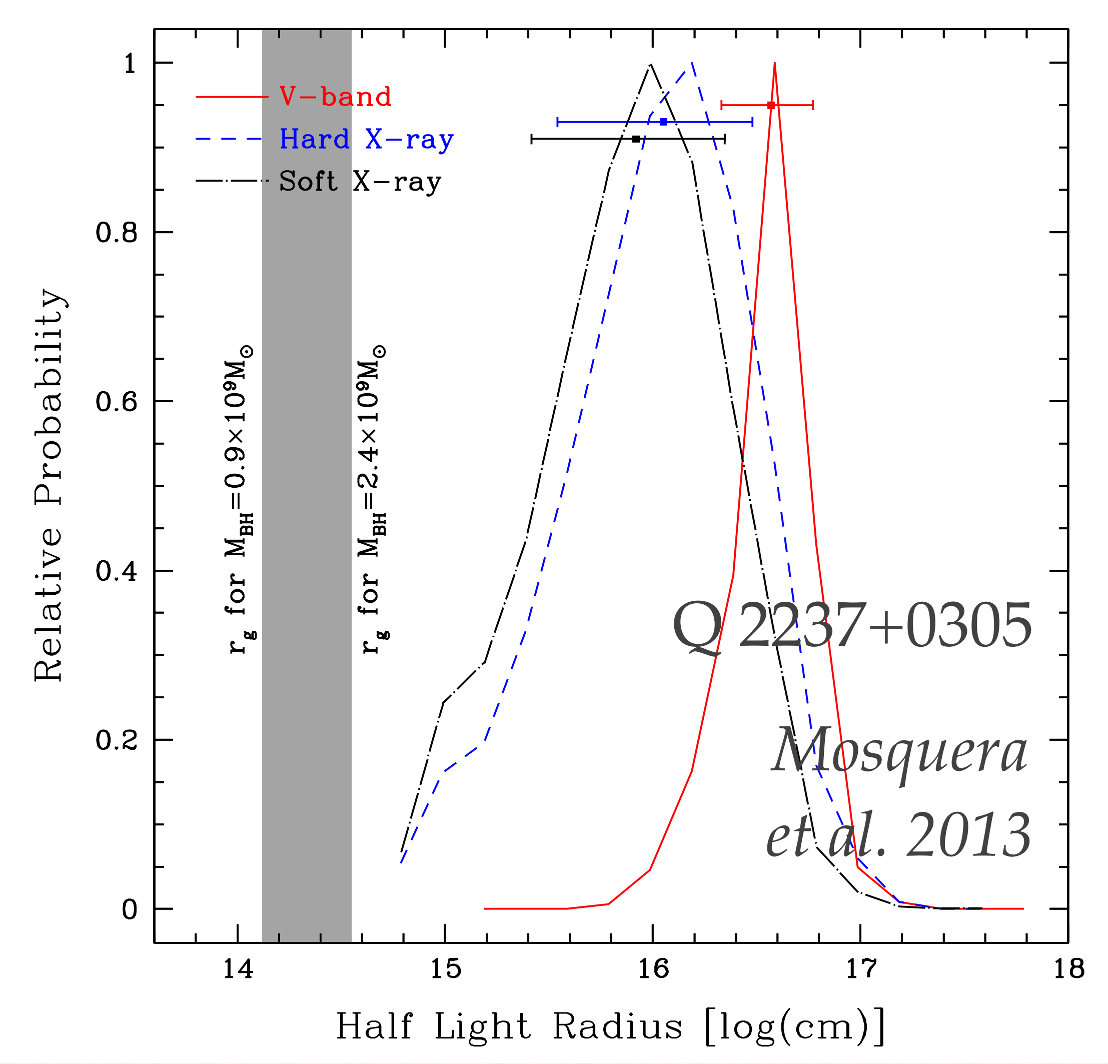

Population

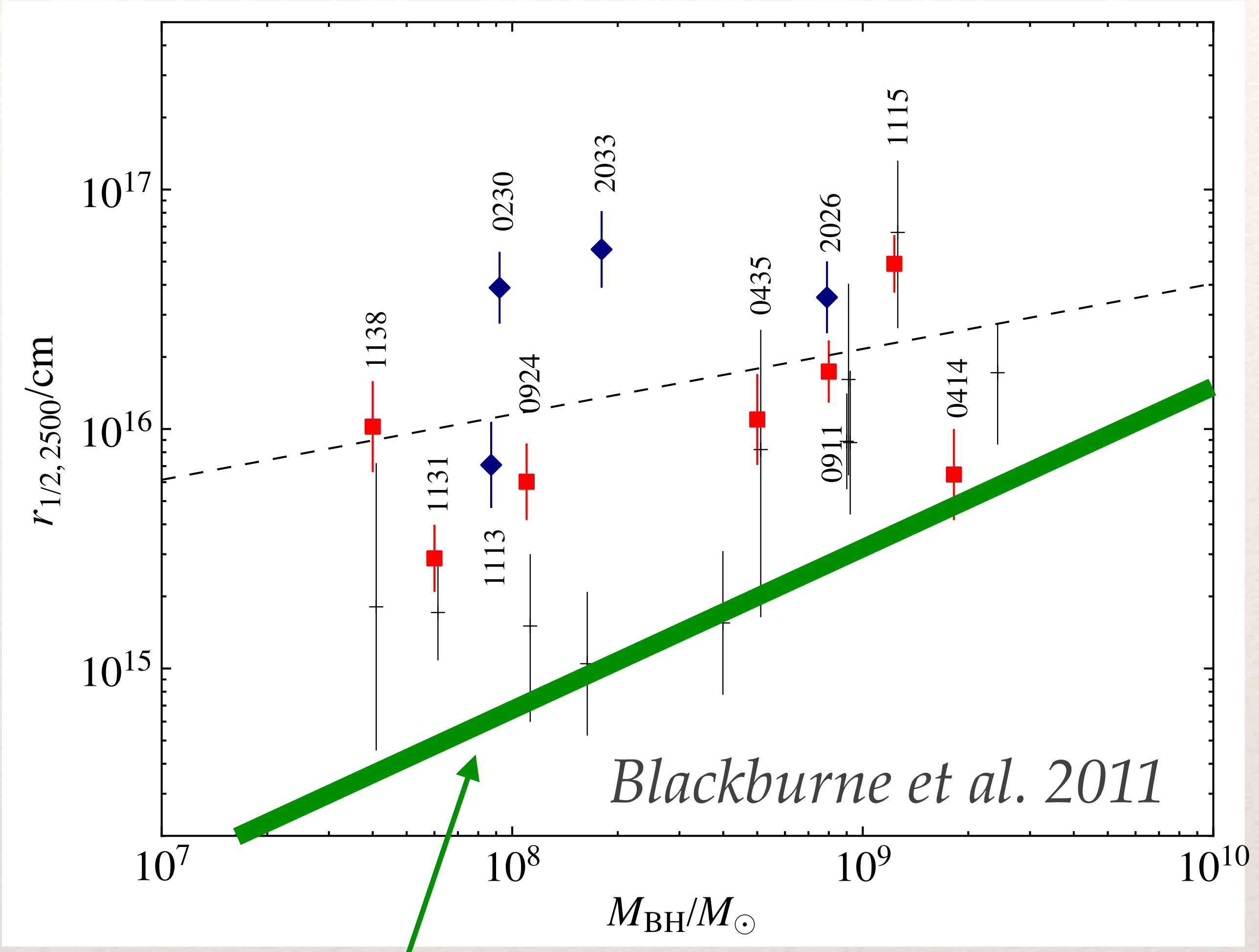

Standard SS Disk

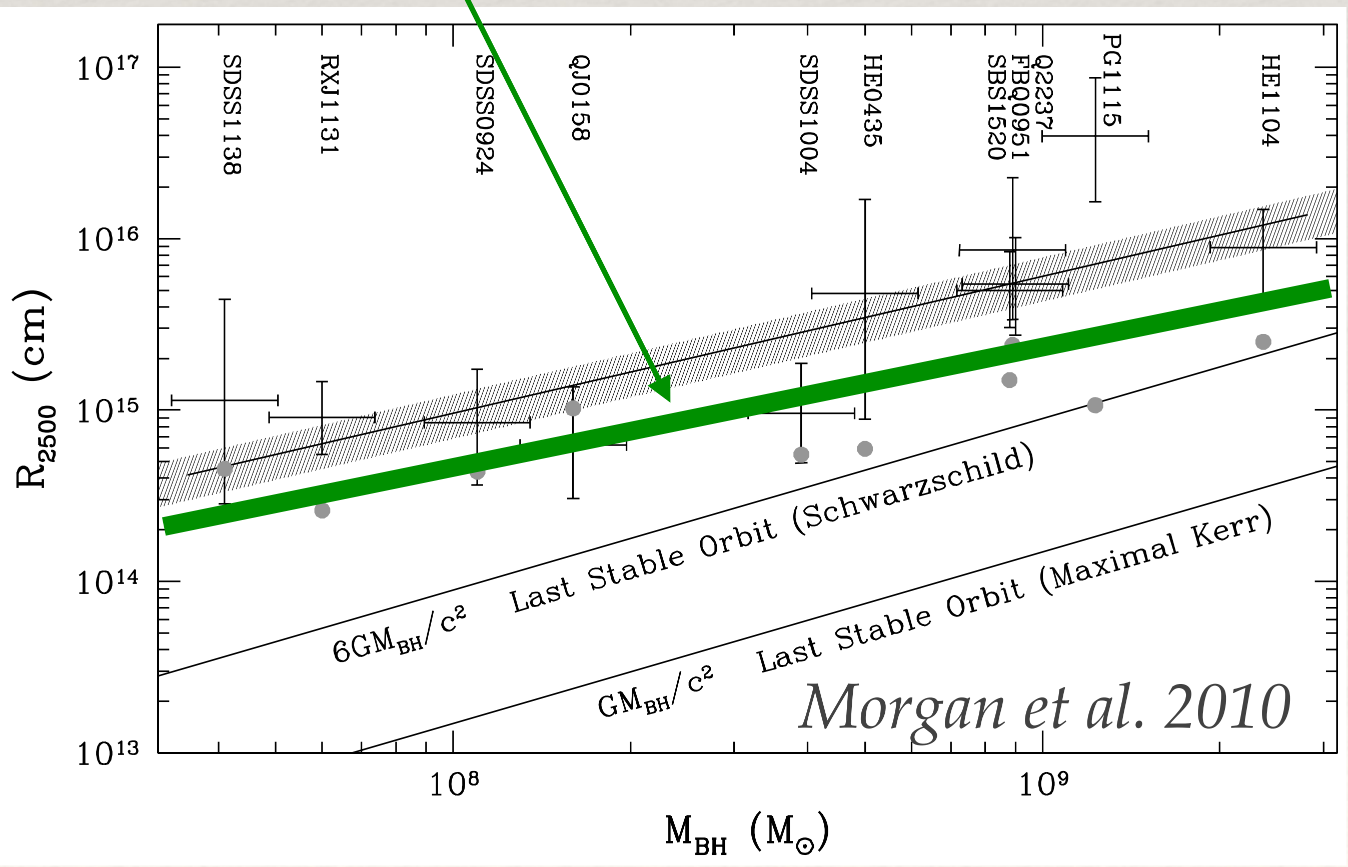

The Anomalies Are Now a **Powerful** Tool

Quasar Structure: micro-lensing of Fe line strongly constrains inner disk.

- Fe line micro-lensing has been observed in several systems (e.g., Chartas et al. 2002; Dai et al. 2003; Ota et al. 2006; Chartas et al. 2007; Chen et al. 2012; Chartas et al. 2012; Chartas et al. 2017)
- Utilizing such observations requires advanced modeling of both strong-field gravity and micro-lensing features (e.g., Heyrovský & Loeb 1997; Popovic et al. 2001, 2003a, 2003b, 2006; Jovanovic et al. 2009; Neronov & Vovk 2016; Krawczynski & Chartas 2017; Ledvina et al. 2018)

RX J1131–1231: $R_{ISCO} \lesssim 9\ R_g$

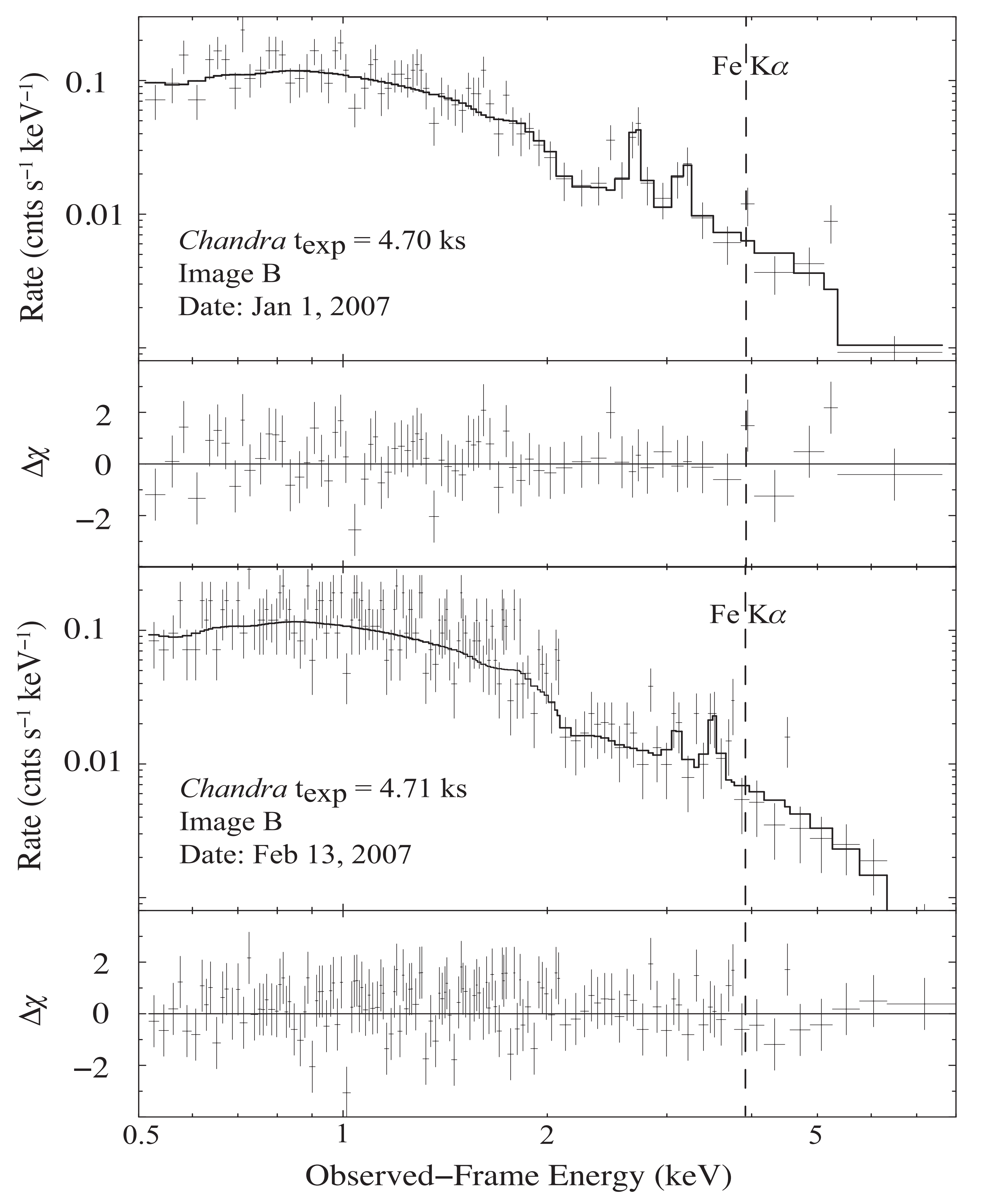

Chartas et al. 2012

Chandra Continues to Solve Mysteries

Lensing galaxy: lensed quasar images are sensitive to dark matter structure

A&A, 685, A15 (2024)
https://doi.org/10.1051/0004-6361/202347689

Astronomy & Astrophysics

The missing quasar image in the gravitationally lensed quasar HE0230−2130: Implications for the cored lens mass distribution and dark satellites

S. Ertl[1,2], S. Schuldt[3,4], S. H. Suyu[1,2,5], P. L. Schechter[6], A. Halkola[7], and J. Wagner[8]

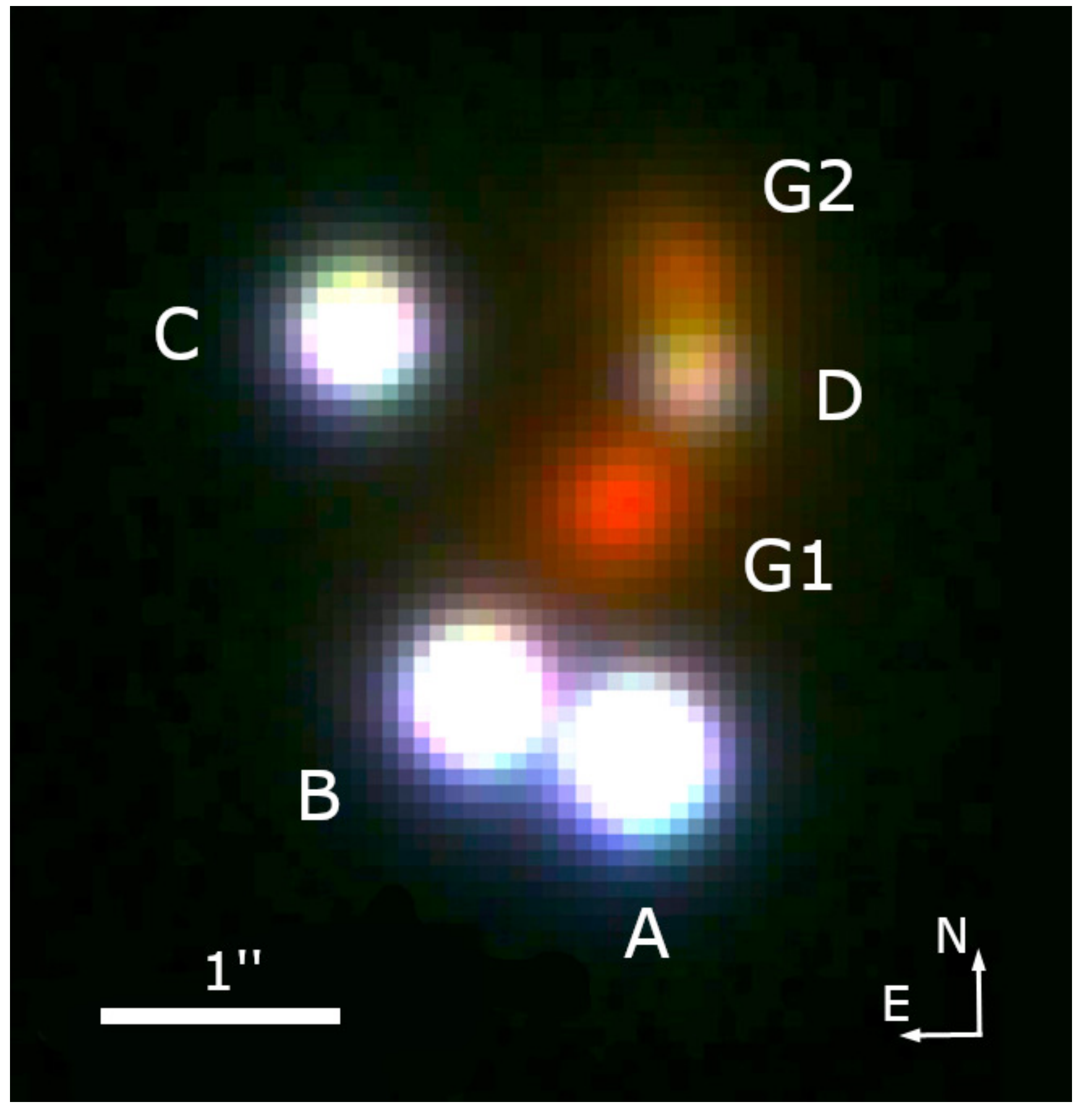

Fig. 1. Color image of HE0230−2130 created with *Magellan* imaging data in the *g*-, *r*-, and *i*-band. Image courtesy of Scott Burles.

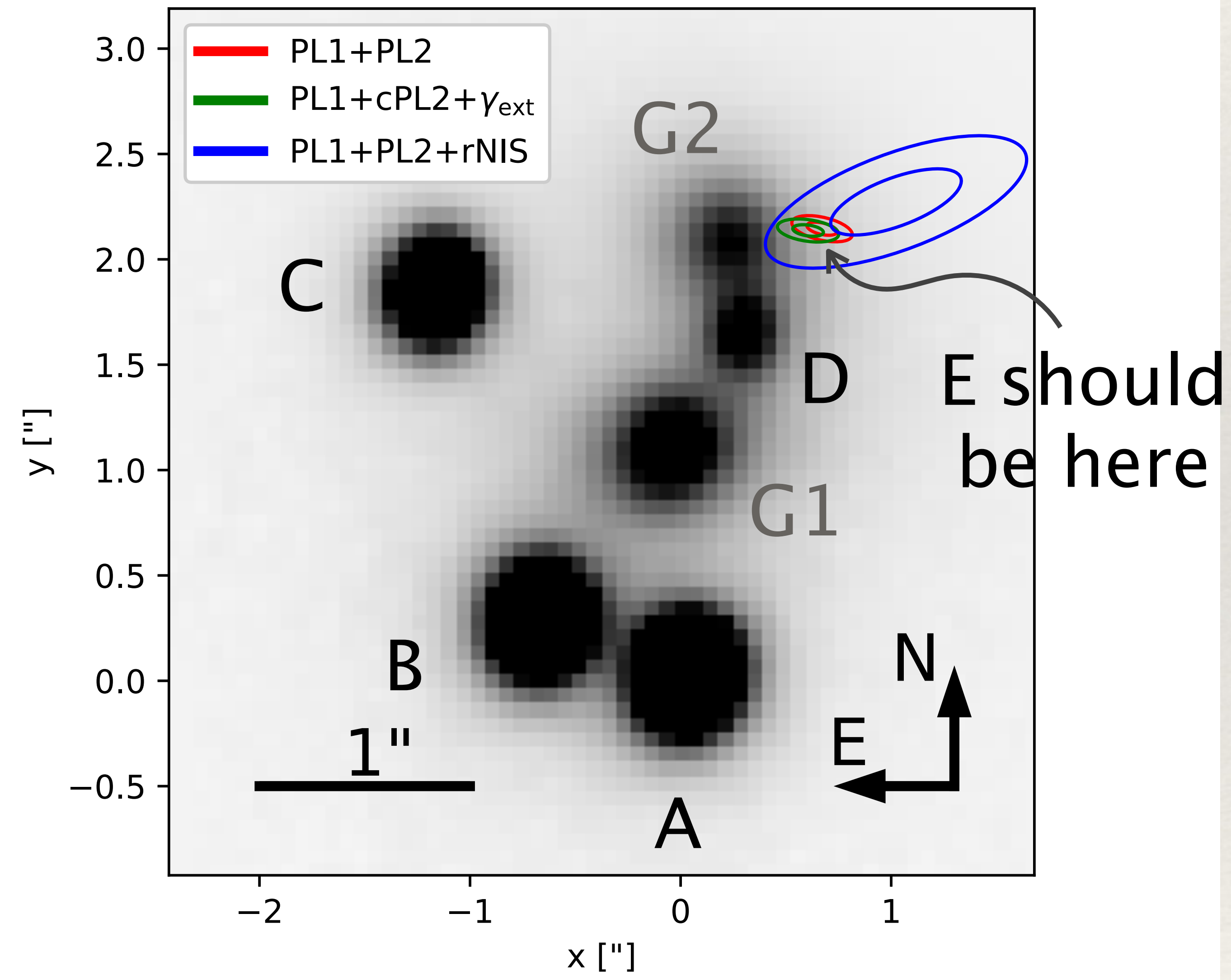

Fig. 3. Modeled image of HE0230−2130. Plotted are the 1σ and 2σ contours of the predicted positions of the unobserved image E in the PL1 + PL2 (red), the PL1+cPL2+γ_{ext} (green), and the PL1+PL2+rNIS (blue) model class. These predicted fifth quasar images would be above the detection threshold, but are not observed in the imaging data.

- Mass models of the two lensing galaxies with standard power-law profiles robustly predict a fifth image which is not seen in deep Magellan or *HST* imaging.
- Twelve different mass models, with increasing degrees of complexity, were investigated to see which could suppress the fifth image.

Table 1. Overview of all 12 model classes.

Model name	Description
PL1 + PL2	G1&G2: singular PL profiles
PL1 + PL2 + γ_{ext}	G1&G2: singular PL profiles, external shear
PL1 + cPL2	G1: singular PL profile, G2: cored PL profile
PL1 + cPL2 + γ_{ext}	G1: singular PL profile, G2: cored PL profile, external shear
cPL1 + cPL2	G1&G2: cored PL profiles
cPL1 + cPL2 + γ_{ext}	G1&G2: cored PL profiles, external shear
PL1 + PL2 + SIS	G1&G2: singular PL profiles, SIS without positional prior
PL1 + PL2 + NIS	G1&G2: singular PL profiles, NIS without positional prior
PL1 + PL2 + rSIS	G1&G2: singular PL profiles, SIS with positional prior
PL1 + PL2 + rNIS	G1&G2: singular PL profiles, NIS with positional prior
PL1 + PL2 + rSIS + γ_{ext}	G1&G2: singular PL profiles, SIS with positional prior, external shear
PL1 + PL2 + rNIS + γ_{ext}	G1&G2: singular PL profiles, NIS with positional prior, external shear

Notes. The positional prior on the SIS and NIS models has a Gaussian distribution and is centred in the region where additional images were predicted.

- All had issues.
- Most plausible one was a non-standard, cored mass distribution for G2.

Chandra Continues to Solve Mysteries

Lensing galaxy: lensed quasar images are sensitive to dark matter structure

A&A, 685, A15 (2024)
https://doi.org/10.1051/0004-6361/202347689

Astronomy & Astrophysics

The missing quasar image in the gravitationally lensed quasar HE0230−2130: Implications for the cored lens mass distribution and dark satellites

S. Ertl[1,2], S. Schuldt[3,4], S. H. Suyu[1,2,5], P. L. Schechter[6], A. Halkola[7], and J. Wagner[8]

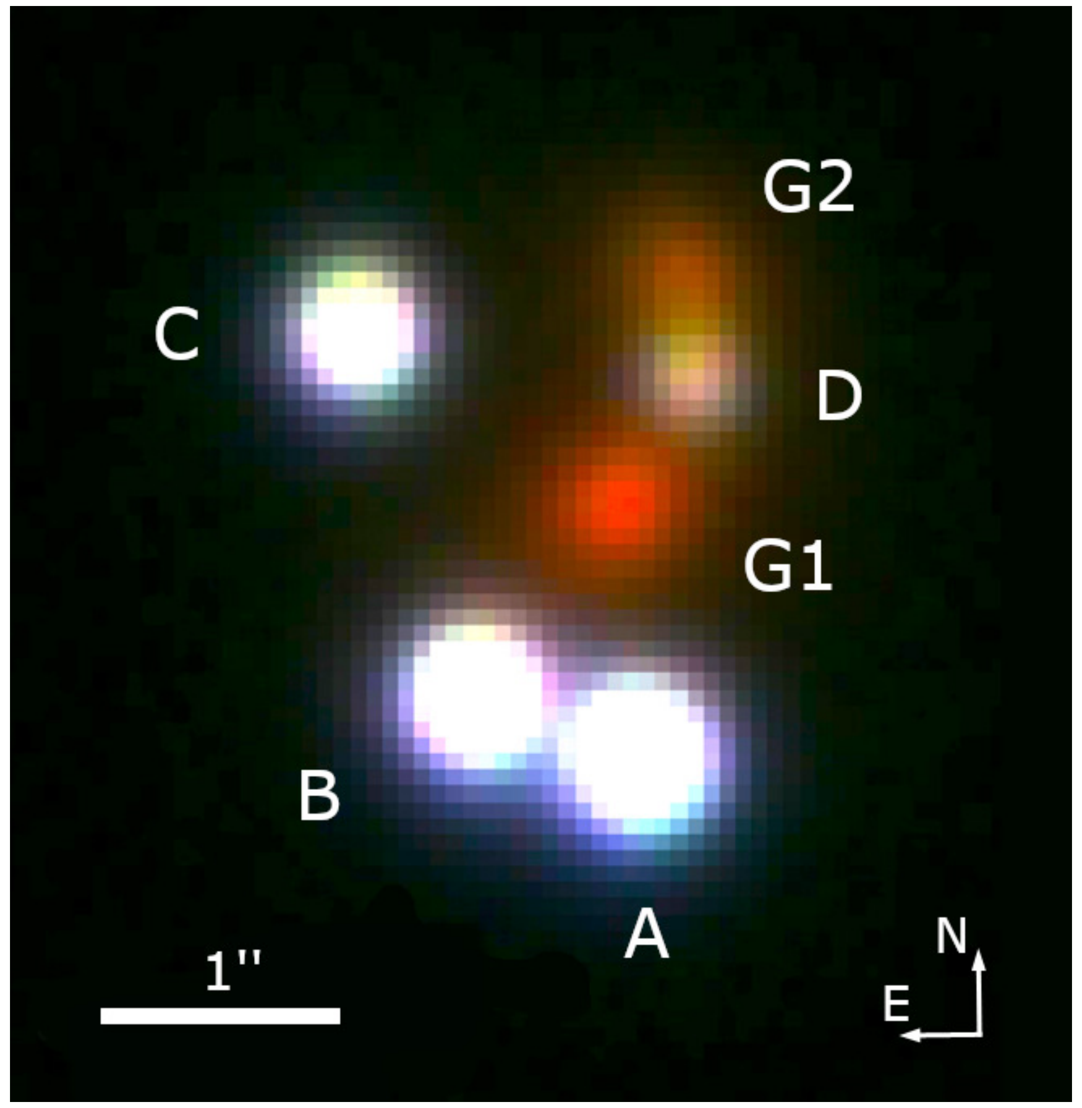

Fig. 1. Color image of HE0230−2130 created with *Magellan* imaging data in the *g*-, *r*-, and *i*-band. Image courtesy of Scott Burles.

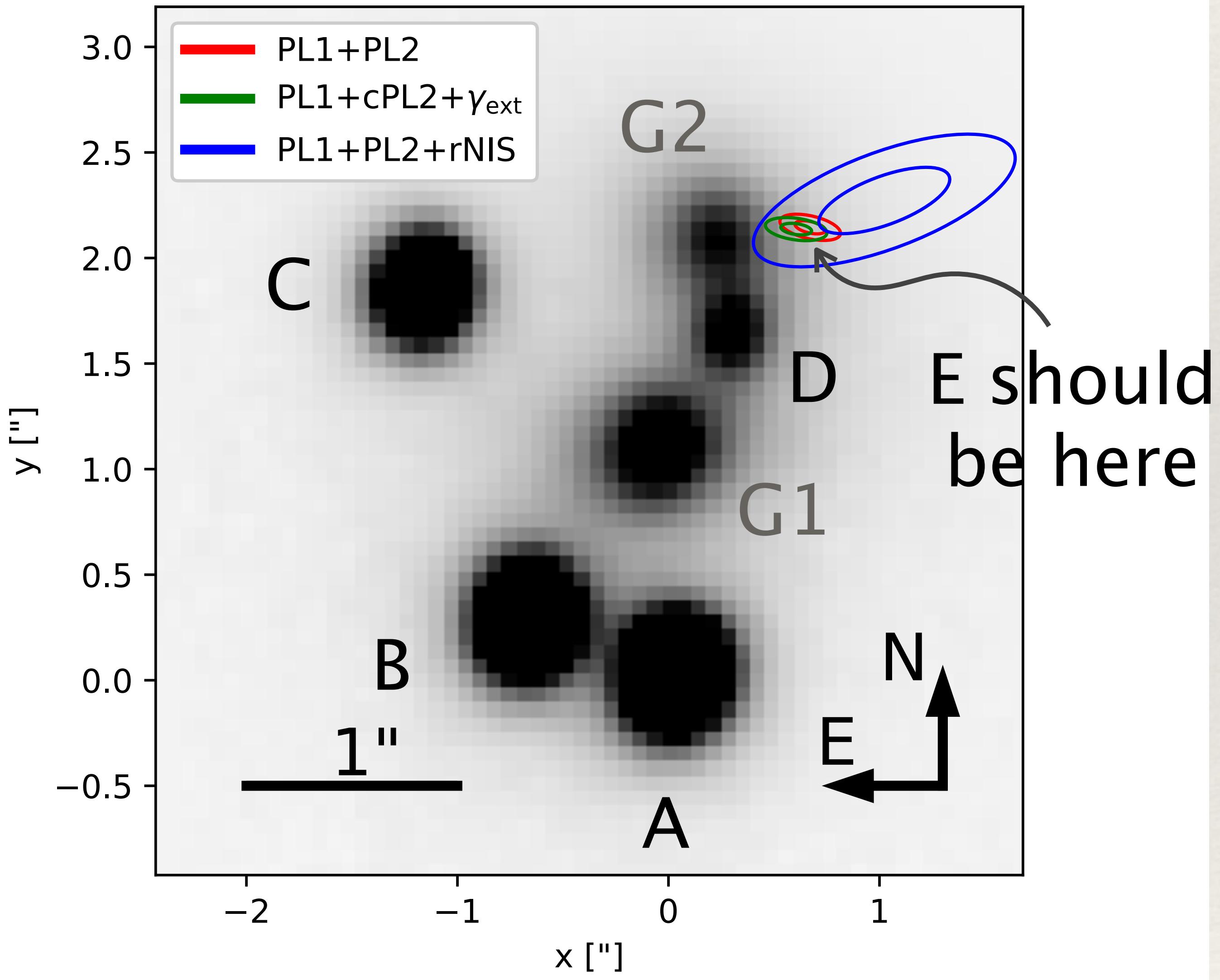

Fig. 3. Modeled image of HE0230−2130. Plotted are the 1σ and 2σ contours of the predicted positions of the unobserved image E in the PL1 + PL2 (red), the PL1+cPL2+γ_{ext} (green), and the PL1+PL2+rNIS (blue) model class. These predicted fifth quasar images would be above the detection threshold, but are not observed in the imaging data.

- Combined Chandra image from eight carefully registered and merged observations (190 ksec total) clearly shows fifth image at expected location from standard mass modeling.

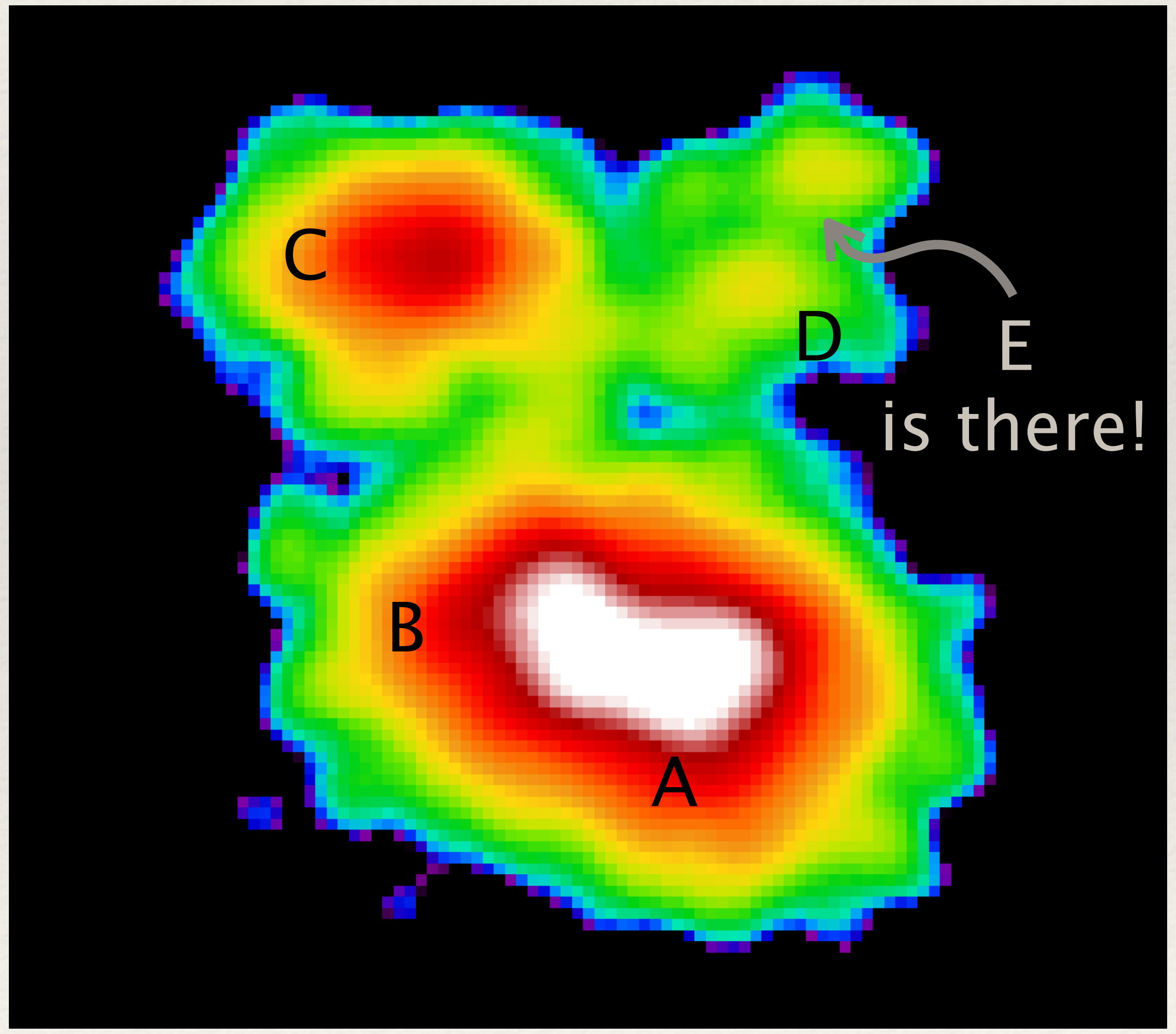

DP, Schechter, et al., in prep.

A Revolution

Chandra's unique and powerful capabilities have resolved several important **long-standing** problems.

Chandra made X-ray observations a **necessary** part of "mainstream" astronomy.